Turun yliopisto
University of Turku

CHARACTERISTICS OF URBAN HEAT ISLAND (UHI) IN A HIGH-LATITUDE COASTAL CITY – A CASE STUDY OF TURKU, SW FINLAND

Juuso Suomi

TURUN YLIOPISTON JULKAISUJA – ANNALES UNIVERSITATIS TURKUENSIS
Sarja - ser. A II osa - tom. 295 | Biologica - Geographica - Geologica | Turku 2014

University of Turku

Department of Geography and Geology
Faculty of Mathematics and Natural Sciences

Supervised by

Professor Jukka Käyhkö
Department of Geography and Geology
University of Turku
Turku, Finland

Reviewed by

Professor Emeritus Timothy R. Oke
Department of Geography
University of British Columbia
Vancouver, Canada

Graduate Director Melissa Hart
ARC Centre of Excellence for Climate
System Science
The University of New South Wales
Sydney, Australia

Opponent

Lecturer Agnieszka Wypych
Department of Climatology
Institute of Geography
and Spatial Management
Jagellonian University
Krakow, Poland

The originality of this thesis has been checked in accordance with the University of Turku quality assurance system using the Turnitin OriginalityCheck service.

ISBN 978-951-29-5911-2 (PRINT)
ISBN 978-951-29-5912-9 (PDF)
ISSN 0082-6979
Painosalama Oy - Turku, Finland 2014

ABSTRACT

The term urban heat island (UHI) refers to the common situation in which the city is warmer than its rural surroundings. In this dissertation, the local climate, and especially the UHI, of the coastal city of Turku (182,000 inh.), SW Finland, was studied in different spatial and temporal scales. The crucial aim was to sort out the urban, topographical and water body impact on temperatures at different seasons and times of the day. In addition, the impact of weather on spatiotemporal temperature differences was studied. The relative importance of environmental factors was estimated with different modelling approaches and a large number of explanatory variables with various spatial scales.

The city centre is the warmest place in the Turku area. Temperature excess relative to the coldest sites, i.e. rural areas about 10 kilometers to the NE from the centre, is on average 2 °C. Occasionally, the UHI intensity can be even 10 °C. The UHI does not prevail continuously in the Turku area, but occasionally the city centre can be colder than its surroundings. Then the term urban cool island or urban cold island (UCI) is used. The UCI is most common in daytime in spring and in summer, whereas during winter the UHI prevails throughout the day. On average, the spatial temperature differences are largest in summer, whereas the single extreme values are often observed in winter. The seasonally varying sea temperature causes the shift of relatively warm areas towards the coast in autumn and inland in spring.

In the long term, urban land use was concluded to be the most important factor causing spatial temperature differences in the Turku area. The impact was mainly a warming one. The impact of water bodies was emphasised in spring and autumn, when the water temperature was relatively cold and warm, respectively. The impact of topography was on average the weakest, and was seen mainly in proneness of relatively low-lying places for cold air drainage during night-time. During inversions, however, the impact of topography was emphasised, occasionally outperforming those of urban land use and water bodies.

Annales Universitatis Turkuensis A II: Biologica, Geographica, Geologica

Turku, 2014

Keywords: urban heat island (UHI), urban cold island (UCI), temperature modelling, land use, topography, water body, seasonality

TIIVISTELMÄ

Kaupungin lämpösaarekkeella tarkoitetaan tilannetta, jossa kaupunkialueet ovat ympäröiviä maaseutumaisempia alueita lämpimämpiä. Väitöskirjassa tarkasteltiin Lounais-Suomessa sijaitsevan rannikkokaupungin Turun (182,000 asukasta) paikallisilmastoa, ja erityisesti lämpösaareketta, erilaisissa alueellisissa ja ajallisissa mittakaavoissa. Lämpötilojen alueellisten erojen osalta keskeisenä tavoitteena oli selvittää, mikä on kaupungin, korkeuserojen sekä vesialueiden vaikutus alueellisiin lämpötilaeroihin eri vuoden- ja vuorokaudenaikoina.

Väitöskirjassa tarkasteltiin lisäksi, miten lämpötilaerojen alueelliset ja ajalliset ominaispiirteet riippuvat säätilasta. Lämpötilaeroihin vaikuttavien tekijöiden voimakkuutta arvioitiin erilaisten mallinnusmenetelmien avulla useita eri selittäviä muuttujia sekä alueellisia mittakaavoja käyttäen.

Kaupungin keskusta on Turussa keskimäärin lämpimintä aluetta. Lämpötilaero kymmenisen kilometriä keskustasta koilliseen sijaitseviin maaseutumaisiin alueisiin on keskimäärin 2 astetta. Suurimmillaan lämpösaarekkeen voimakkuus voi olla kymmenenkin astetta. Lämpösaareke ei vallitse Turussa jatkuvasti, vaan ajoittain kaupungin keskusta saattaa olla ympäristöään viileämpi. Tällöin puhutaan kylmäsaarekkeesta. Kylmäsaareke siintyy yleisimmin päiväsaikaan keväällä ja kesällä, kun taas talvella lämpösaareke vallitsee tavallisesti vuorokaudenajasta riippumatta. Alueelliset lämpötilaerot ovat keskimäärin suurimmillaan kesällä, kun taas yksittäiset ääriarvot saavutetaan usein talvella. Meriveden lämpötila vaikuttaa lämpösaarekkeen painopisteeseen siten, että se siirtyy syksyllä kohti rannikkoa ja keväällä kohti sisämaata.

Kaupunkimaisen maankäytön todettiin olevan pitkällä aikavälillä merkittävin alueellisia lämpötilaeroja aiheuttava tekijä. Vaikutus oli pääasiassa lämpötiloja nostava. Vesialueiden vaikutus korostui keväällä veden lämpötilan oltua suhteellisen alhainen, sekä syksyllä veden lämpötilan oltua suhteellisen korkea. Korkeuserojen vaikutus oli keskimäärin vähäisin, ja ilmeni lähinnä alavien paikkojen alttiutena öiselle kylmän ilman valumiselle. Inversiotilanteissa topografian merkitys kuitenkin korostuu, ja sen vaikutus on ajoittain kaupungin ja vesialueiden vaikutusta suurempi.

Annales Universitatis Turkuensis A II: Biologica, Geographica, Geologica.

Turku, 2014

Avainsanat: kaupungin lämpösaareke, kaupungin kylmäsaareke, lämpötilojen mallintaminen, maankäyttö, topografia, vesialueet, vuodenaikaisuus

ACKNOWLEDGEMENTS

The PhD project has proceeded from its absolute zero point to its end. Along the journey, there have been many milestones that reach back to the end of the last millennium. At the end of 1990ies, Sakari Tuhkanen, professor of physical geography at the University of Turku, started to plan the urban climate observation network to the coastal city of Turku and its surroundings in southwestern Finland. From the very early phases of the planning process, Jukka Käyhkö, the present professor of physical geography, and the supervisor of this thesis, has been a key person in planning and implementing the urban climate measurements, which materialised as the first observations in spring 2001. The project was named "Turku Urban Climate Research Project (TURCLIM)". Measurements have continued until today, and are planned to continue to the indefinite future. While the preliminary idea of Sakari Tuhkanen has been the starting point of the project, further coordination by Jukka Käyhkö has kept the TURCLIM project running, enabling e.g. the completion of this thesis. Jukka's contribution as a supervisor and co-author has been essential during the PhD project. In addition to the impact on the contents of this thesis, discussions with him have also raised many additional ideas that wait to be implemented.

I would like to thank the co-author of papers III and IV, Jan Hjort, professor of physical geography, from the Department of Geography at the University of Oulu. Jan's strong statistical expertise and novel ideas concerning spatial modelling of temperatures have capitalised in two published articles, and the collaboration will hopefully continue also in the future. In addition to the contributions by the co-authors, the published articles of this thesis have been refined by comments and suggestions made by anonymous reviewers of the manuscripts. The PhD manuscript and the unpublished article manuscript have been improved by the valuable comments of the pre-examiners, Dr., Professor Emeritus Timothy R. Oke and Dr., Graduate Director Melissa Hart.

Professor Risto Kalliola, Head of the Department of Geography and Geology, has successfully navigated the geography community through sometimes stormy waters of organisational reform. Special thanks to Risto as head of department for guaranteeing the continuity of weather observations in Turku by his decision to maintain the TURCLIM project with essential contribution from the department. Thanks also to the other PhD students and personnel of the department. The morning coffee has been a good social way to start the working day. In general, discussions with colleagues have been fruitful and refreshing during the PhD marathon, regardless of whether the topic has dealt with work or something else.

Many people have participated in the data collection of this thesis. The data period starts from 2002, and at the beginning, Albert Driesprong and Tuomas Einiö read the

weather devices. They also installed the measurement network in 2001. From 2004 up to 2007, I collected the data mostly with Raisa Murtovaara. From 2004 onwards also Jani Helin, Niko Humalisto, Minna Huovinen, Paulina Nordström, Mika Orjala, Arto Peltola, Rauno Varjonen and Risto Väyrynen have participated in the field work. The 'climate tours' have offered plenty of comical situations, and often the field days have not felt like work at all.

TURCLIM project collaborates with the Turku Environment and City Planning office. Their assistance has covered a broad range extending from financial co-operation to collaboration in teaching and research. Special thanks go to Stella Aaltonen, Mikko Jokinen, Miika Meretoja and Olli-Pekka Mäki for preparing the possibilities to utilise and apply the research results in a real-world framework, i.e. in urban planning. My PhD project has been integrated in the project "Climate-Proof City (ILKKA) – Tools for Planning" financed by the European Regional Development Fund, which has taken steps towards a more concrete application of the information on spatial temperature differences. During the PhD process, the collaboration with the Finnish Meteorological Institute has increased from the early steps taken in 2009. I would like to thank Achim Drebs, Hilppa Gregow and Antti Mäkelä for co-operation in the ILKKA project and Achim also for longer research collaboration, joint teaching and discussions of urban climate. The TURCLIM measurement devices have been renewed in 2010. I would like to thank Tom Kuusela and Juha Peura at the Department of Physics and Astronomy for offering room to calibrate the new devices.

Financing of the thesis has come in the form of personal scholarships from three foundations; Emil Aaltonen Foundation, the Finnish Cultural Foundation's Varsinais-Suomi Regional Fund, and Turku University Foundation. The financing has been necessary in enabling the concentration on the research.

Thanks to my friends. The majority of discussions with you has dealt with something else than work, which has helped me better concentrate on the research when needed. Special thanks to my mother Anneli, her spouse Allu, father Kari, sister Salla and her family. My parents and sister probably remember my interest in weather already in childhood, as our house was equipped with many thermometers I had installed. At that time, observing the weather was more spontaneous and did not feel like work, which it has occasionally felt during the PhD process.

TABLE OF CONTENTS

LIST OF ORIGINAL PUBLICATIONS

This thesis consists of the summary and the following papers, which are referred to in the text by their Roman numerals:

I Suomi, J., Käyhkö, J. (2012). The impact of environmental factors on urban temperature variability in the coastal city of Turku, SW Finland. International Journal of Climatology 32: 451-463.

II Suomi, J. Spatial and temporal characteristics of urban heat island during different weather patterns – a case study in Turku, SW Finland. Submitted manuscript.

III Hjort, J., Suomi, J., Käyhkö, J. (2011). Spatial prediction of urban-rural temperatures using statistical methods. Theoretical and Applied Climatology 106 (1-2): 139-152.

IV Suomi, J., Hjort, J., Käyhkö, J. (2012). Effects of scale on modelling the urban heat island in Turku, SW Finland. Climate Research 55: 105-118.

1. INTRODUCTION

Urban climate

The climate of an urban area often differs from that of the surrounding countryside. One of the features of urban climate is the *urban heat island* (UHI), which appears as the relative warmness of a city (Oke, 1987). The UHI is commonly defined as the temperature difference between urban and rural location (e.g. Kolokotroni et al., 2010; Steeneveld et al., 2011; Emmanuel and Krüger, 2012) or *spatially averaged* temperature differences between urban and rural areas (e.g. Kolokotroni and Giridharan, 2008). Although a city is typically warmer than its surroundings, occasionally the pattern is reversed, and the city centre is colder than the outskirts (e.g. Klysik and Fortuniak, 1999). In this case, the term *urban cold island* or *urban cool island* (UCI) is used (e.g. Steinecke, 1999; Li et al., 2011). The UHI phenomenon affects an increasing number of people as a result of rapid global urbanisation (WHO, 2013).

Luke Howard's study of the climate of London, published in 1818, is often considered the starting point of UHI research. The severe air quality problems of London – the infamous smog – had already been considered earlier, but in his study, Howard was able to demonstrate that the city centre was not only more polluted, but also warmer than the surrounding countryside. Until the middle of the twentieth century, urban climate research was quite descriptive, but it has gradually become more analytic, and the focus has increasingly shifted to understanding and quantifying the processes that create the urban climate (Landsberg, 1981; Souch and Grimmond, 2006; Erell et al., 2011). Measuring technology has also developed. Temperature data have traditionally been collected by stationary measurement networks (e.g. Hinkel et al., 2003), or by portable thermometers (e.g. Yamashita, 1996). Recently airborne and satellite-based remote sensing has also been increasingly utilised in urban climate research (e.g. Voogt and Oke, 2003; Weng, 2009).

How does urban climate form?

Today, the main factors behind UHI are rather well understood. These include the differences in solar heat storage, anthropogenic heat release and evaporation between urban and rural areas. During the daytime solar heat is stored in building structures and pavements. Urban construction materials often have high heat capacity and good thermal conductivity, enabling radiative energy to be stored in a thick layer in urban structures. The stored heat is released in the form of long wavelength radiation (sensible heat) through the evening and night, resulting in a slower cooling of urban areas at night-

time (Landsberg, 1981; Oke, 1987; Cotton and Pielke, 1995). Therefore, UHI is often strongest at night.

Anthropogenic heat is an add-on to the solar radiation balance, released from traffic, industrial activities and the heating/cooling of the buildings. A small proportion of anthropogenic heat is also produced directly by human body metabolism (see e.g. Magee et al., 1999; Fan and Sailor, 2005).

Evaporation differences emerge from the low capacity of urban surfaces to absorb water, and the sewage network that effectively conveys the excess water away. This results in a lower proportion of evaporation in urban areas (Oke, 1987; Wypych, 2010). Consequently, a greater proportion of energy in a city is in sensible form. In rural areas, due to the often larger amount of vegetation, water transfer to the atmosphere also from deeper in the ground via transpiration is effective, supporting the transformation from sensible to latent heat (Oke, 1987; Cotton and Pielke, 1995). Weather has an effect on the UHI intensity: calm and cloudless conditions favour large temperature differences (Oke, 1987). The effect of wind speed is often considered more important than that of cloud cover, but the results are not, however, coherent (Morris et al., 2001).

What are the consequences of urban climate?

How should we consider the presence of UHI? Is it a problem, or a benefit? Indeed, UHI can have neutral, disadvantageous or beneficial consequences depending on the type and location of the city, plus the stakeholders and sectors under consideration. Due to higher temperatures, the growing season is longer in urban areas, and plants start to flower earlier in spring (Steinecke, 1999; NASA, 2004; Lu et al., 2006; Jochner et al., 2012). Urban areas can also be thermally more favourable habitats for some animals (Oke, 1987; Parris and Hazell, 2005). In low latitudes, where temperatures are in general high, the UHI worsens the adverse health effects of heat stress. UHI is typically strongest during calm weather, coinciding with air quality problems amplified due to poor mixing. Higher urban temperatures also promote the formation of secondary pollutants such as ozone (O_3) (Solecki et al., 2004). Although higher urban temperatures alone can increase mortality (e.g. Buechley et al., 1972; Conti et al., 2005; Vaneckova et al., 2008; Matzarakis et al., 2011), the combined effect of UHI-boosted heat stress and poor air quality is a serious problem in low latitudes, especially in summer. Consequently, the UHI increases energy consumption needed for cooling (Priyadarsini et al., 2008; Vardoulakis et al., 2013), and this disadvantage is naturally also most relevant in low latitudes. In high latitudes, in contrast, the UHI can have economically and environmentally beneficial effects due to lower energy demand for heating (Oke, 1987; Taha, 1997; Giridharan and Kolokotroni, 2009). In a nutshell, the negative effects of UHI are mostly concentrated on low latitudes, and positive effects on high latitudes. However, as the climate change

proceeds, heat stress is expected to become a more concrete problem also in high-latitude cities (e.g. Thorsson et al., 2011; Emmanuel and Krüger, 2012).

The adverse effects of UHI have influenced the geographical and seasonal pattern of UHI research; the majority of UHI studies have been conducted in summer and in latitudes lower than that of Turku (60°N), the city studied in this thesis. The technical challenges in temperature measurements in winter have probably also channelled UHI studies towards warmer conditions (Giridharan and Kolokotroni, 2009). Different mitigation and adaptation solutions, such as reflective materials and green rooftops, are common in the climate zones prone to UHI-based exacerbation of heat stress (e.g. Akbari and Konopacki, 2004; Gago et al., 2013; Lee et al., 2013). In high latitudes, heat stress is a serious health risk only during summertime heatwaves (Näyhä, 2007), and only minor UHI mitigation and adaptation measures have been undertaken in these areas. Even if climate change were to increase the need to suppress summertime UHI, the mitigation and adaptation measures could increase the need for wintertime heating (Akbari and Konopacki, 2004), a fact that should be taken into account in decision making. In addition to the possibly increasing need for UHI mitigation measures in the future, the information on local climate can be utilised in various sectors of city planning, e.g. the coldest places are suitable for ice-hockey rinks, while it is inappropriate to locate hospitals and residential areas for elderly people in the regions that are the warmest during heatwaves.

Urban climate research

The quantification of the urban effect on temperature is simplified when the effects of other affecting factors are minimised, e.g. in a flat inland city the effect of water bodies and topography are eliminated (Oke, 1973; Siu and Hart, 2013). In many cities, however, these 'ideal' conditions are not met, and the thermal effects of non-urban and urban environmental factors have been estimated with various modelling and interpolation methods, where temperature has been the dependent variable and environmental factors have been used as explanatory variables (e.g. Eliasson and Svensson, 2003; Hart and Sailor, 2009; Szymanowski and Kryza, 2009). Environmental variables have often been calculated within a certain distance from the temperature observation point or the modelled spatial unit, such as raster or vector grids. The size of the area affecting the weather observation site is not constant and depends, for example, on building density and measurement height. Oke (2006) concludes the 'circle of influence' to be around 500 m for screen-level measurements. In UHI studies, a relatively large variation of buffer sizes has been applied to quantify the environmental factors, extending from tens of metres to up to over 1000 m (e.g. Giridharan et al., 2008; Wen et al., 2011).

The temporal scale of UHI studies has extended from momentary situations to long-term average conditions, depending on the measurement methods and detailed study questions. From a city planning perspective, long-term climatic conditions are often important, whereas health problems tend to be emphasised during certain momentary or short-term weather events (Eliasson and Svensson, 2003; Lai and Cheng, 2009). UHI often has diurnal and seasonal regularities that tend to smooth or vanish when long-time average temperatures are used. Thus, average temperatures of a certain time of day (Giridharan and Kolokotroni, 2009) or of daily minimum or maximum temperatures (Wilby, 2003) have been used to take into account the diurnal UHI variation. In seasonal analyses, month (e.g. Jongtanom et al., 2011) or combinations of several months (Eliasson and Svensson, 2003) have been used as reference periods, and in particular the dichotomy between winter and summer UHI is common (e.g. Oke and Maxwell, 1975; Kolokotroni and Giridharan, 2008; Giridharan and Kolokotroni, 2009). In winter, the role of anthropogenic heat release in the formation of UHI formation is large compared to that of solar radiation, whereas in summer, the situation is often the opposite (Klysik and Fortuniak, 1999; Hamilton et al., 2009). Depending on the city, the dominance of either anthropogenic heat or solar radiation in UHI formation can create two clearly different UHI patterns in the same city, and therefore the summer–winter dichotomy is often justifiable. Emphasis on the adverse effects in summer and the beneficial ones in winter also divides the research settings. Using short-time case studies, or longer study periods split and classified as combinations of similar cases, is common in the research concentrated on the connections between the UHI and weather (Morris and Simmonds, 2000; Zhang and Chen, 2013).

Rationale of the study

At the latitude of the present study area, Turku, 60 °N, seasonal differences in solar radiation are large; in summer, the daily energy content of insolation is approximately 11–12 kWh/m^2, whereas in winter, the corresponding value is only around 0.6–0.7 kWh/m^2 (FAO, 1983; Barry and Chorley, 1998; Strahler and Strahler, 2006). The energy demand for summertime cooling is remarkably lower than that for wintertime heating, causing the peak values of anthropogenic heat to occur in winter (see e.g. Klysik, 1996). As a consequence of the contrasting seasonal rhythm in the energy flux by solar radiation and by anthropogenic heat, the separation of winter UHI from summer UHI is justifiable in research settings in the Turku area. In addition, the rhythmic cooling and warming effects of the sea cause a clearly distinct local climate in autumn and spring in the coastal areas, and thus there is a good reason to study all four seasons. Seasonal comparisons in this study are carried out mainly on a monthly basis.

In the field of urban climate research, this study aims to provide detailed, novel information on the spatio-temporal characteristics of UHI in the high-latitude (60 °N)

coastal city of Turku (182,000 inhabitants). On the one hand, the coastal location and undulating relief of Turku set a challenge to estimating the pure urban effect on spatial temperature differences. On the other hand, however, these geographical features allow the development of methods to distinguish the heating effect of the city from the non-urban affecting factors. In this dissertation, the focus is on the seasonal and diurnal variation in the relative importance of environmental factors causing the UHI in the area. The scale of these environmental factors is also explored, as well as the connections between the UHI and weather (Figure 1). The main aims of this thesis can be summarised as:

(i) unravelling the seasonal and diurnal behaviour of UHI in the mid-size high-latitude coastal town of Turku;

(ii) analysing the connections between spatio-temporal temperature variation and weather;

(iii) testing and assessing the applicability of various statistical methods in spatio-temporal UHI modelling;

(iv) distinguishing the actual urban effect from other local climatic factors in the formation of UHI, and

(v) analysing and determining the circle of influence of various environmental variables.

Objective (i) is tackled mainly in papers **I** and **II**. Paper **I** produces information on the long-term spatio-temporal temperature variation, while paper **II** concentrates on shorter timescales. In paper **I**, the seasonal variation of temperatures is studied on a monthly basis, and in paper **II**, with one-week-long study periods, two of which are in the summer and two in the winter. The long-term regularities in the diurnal temperature variation are unravelled by comparing the spatial temperature differences in the average temperatures, daily minimum temperatures, daily maximum temperatures and diurnal temperature ranges (**I**). A more detailed pattern of diurnal temperature variation is gained in paper **II** by analysing the temperature variation at half-hour intervals.

Objective (ii) is considered in paper **II**. The one-week-long study periods were selected based on different synoptic-scale weather conditions. In addition, the dependence between (a) UHI and wind speed and (b) UHI and cloudiness were examined on a yearly basis. In winter, the first study period was dominated by high pressure, low wind speeds, low cloudiness and colder-than-average conditions, whereas during the latter study period, low pressures dominated and the weather was windy, cloudy and mild. In summer, the first study period was dominated by low pressures, and the latter by high

pressures. Consequently, the weather was windier, cloudier and colder during the first study period.

Objective (iii) is unravelled in papers **I**, **III** and **IV**. In paper **I**, the environmental variables were determined and quantified based on various *geographic information systems* (GIS) methods. Thereafter, the relative importance of the variables were estimated with correlation analysis (**I**; **IV**), hierarchical partitioning (HP) (**IV**), linear regression (LR) (**I**; **IV**), boosted regression trees (BRT) and a generalised linear model (GLM) (**III**). An estimation was made for annual (**I**) and monthly average temperatures (**I**; **III**; **IV**), monthly averages of daily minimum temperatures, daily maximum temperatures and diurnal temperature ranges (**I**; **III**).

Objective (iv) is tackled in all four papers. In paper **I**, the impact of urban land use is compared with the effects of water bodies and topography using correlation analysis and a linear regression model. The relative strengths of urban and non-urban environmental factors were assessed using a *generalised linear model* (GLM) and *boosted regression tree* (BRT) methods in paper **III** and using *hierarchical partitioning* (HP) and a *linear regression* (LR) model in paper **IV**. In the above-mentioned modelling settings the impacts of urban and non-urban environmental factors were estimated against long-term average temperatures (including monthly averages of daily minima, maxima and diurnal temperature range). In a shorter timescale, the impacts of urban and other environmental factors were estimated in paper **II**.

Objective (v) is in the focus in paper **IV**, in which the optimal circle of influence area is estimated using correlation analysis. The estimation is made for urban and non-urban environmental variables on a monthly basis. The variables with the optimal buffer sizes are applied in the following phases of the paper. Firstly, the strongest urban variable was screened from the potential, but intercorrelated variables using HP. Secondly, the independent effect of the strongest urban variable was compared with that of the non-urban variables, again using HP. Finally, the relative importance of the environmental variables was assessed using a linear regression model.

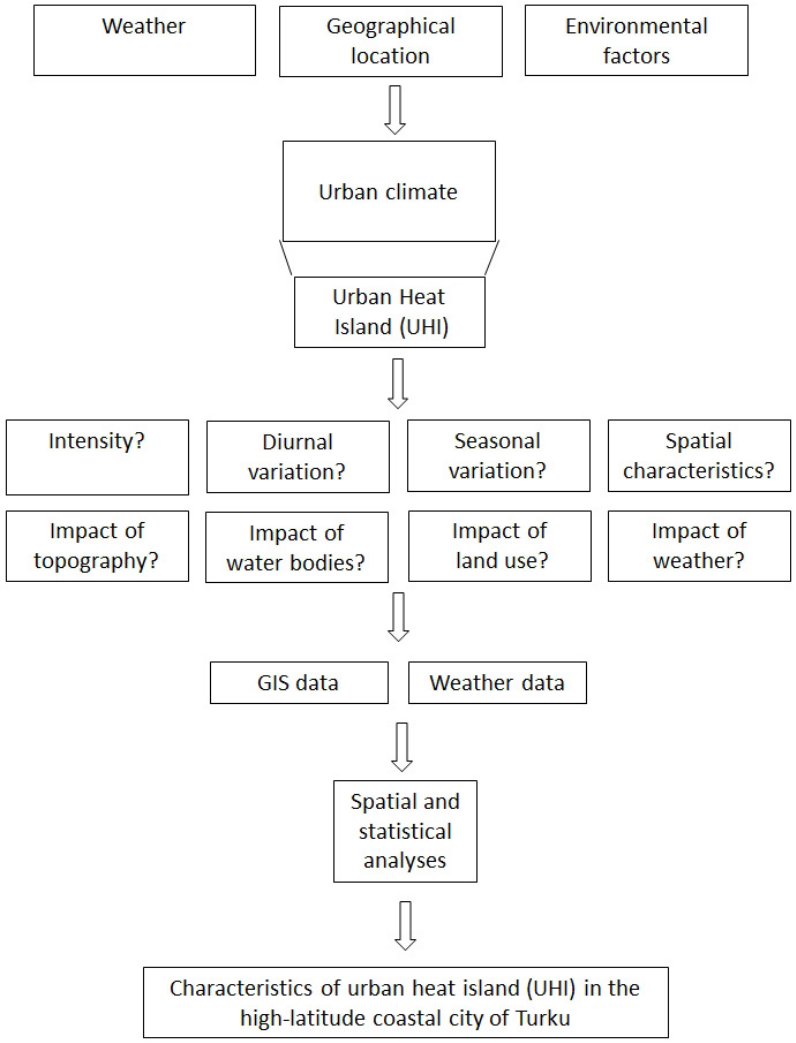

Figure 1. Theoretical and methodological framework of the thesis. The specified research questions derive from the objectives (i) – (v).

2. THEORETICAL BACKGROUND

UHI can be defined for different layers in the atmosphere. *Canopy layer UHI* refers to the heat island observed between the surface and rooftop level, whereas *boundary layer UHI* means the heat island extending vertically from the rooftop level up to the height where the city effect still exists (Oke, 1976). The UHI can also be determined for the land surface, and in this case the term *surface urban heat island (SUHI)* is used. The measurement of canopy layer UHI is often done with *in situ* sensors at the standard measurement height, i.e. around 2 metres' elevation. Mobile measurements with vehicle-mounted sensors are also common. The boundary layer UHI is often recorded with sensors installed in high towers. Balloon flights and aircraft-mounted sensors are also utilised. The SUHI is often recorded with remote sensors (Voogt and Oke, 2003). The benefit of the *in situ* canopy and boundary layer UHI measurement methods is the possibility of making observations at high temporal resolution, but the spatial resolution is often poorer than with remote sensing methods (Streutker, 2003). In the methodology and literature review of this thesis, the focus is on the canopy layer UHI.

The differences in energy fluxes between urban and rural areas are manifested in their particular local climates. The energy balance of a certain area can be divided into various components. Oke (1987) represents the energy balance of a building-air volume with the equation:

$$Q^* + Q_F = Q_H + Q_E + \Delta Q_S + \Delta Q_{A,} \quad (1)$$

where:

Q^* = net all-wave radiation flux density
Q_F = anthropogenic heat flux density due to combustion
Q_H = turbulent sensible heat flux density
Q_E = turbulent latent heat flux density
Q_S = sensible heat storage
Q_A = horizontal energy transport in the air per unit horizontal area

The equation can be simplified in the form:

$$Q^* = Q_H + Q_E + \Delta Q_S \quad (2)$$

by incorporating the anthropogenic heat flux into the other terms and by assuming ΔQ_A to be negligible or non-existent (see Cleugh and Oke, 1986). In evapotranspiration, the energy is absorbed in the water vapour as latent heat, and the term Q_E equals evapotranspiration in the equation (2). Of all energy balance components, the most significant urban–rural

differences are in the daytime heat storage and evapotranspiration, the former being larger in urban areas and the latter in rural areas. In addition, anthropogenic heating is a noteworthy surplus in energy flux in urban areas (Oke, 1987; Christen and Vogt, 2004). In the following, the items of energy balance crucial for UHI are discussed in more detail.

2.1 Thermophysical determinants of UHI

2.1.1. Differences in radiation

Solar radiation is by far the most important source of energy on the Earth. Excluding the filtering effect of the atmosphere, the amount of energy received at a certain point depends on solar activity, the distance from the sun, sun altitude and day length. The Sun irradiates energy at wavelengths between 0.15 and 4 μm, with the maximum energy flux density at 0.5 μm (blue-green). The solar constant, i.e. the flux density of the solar radiation at the top of the atmosphere, is approximately 1370 W/m^2. The wavelength of the radiation emitted by the Earth extends from 3 μm to 100 μm, the maximum intensity being at 10 μm. Less than 1% of the radiation emitted by the Earth and Sun overlaps between 3–4 μm, and the wavelength of 4 μm is often considered a division between short wave and long wave, or solar and terrestrial, radiation (Geiger et al., 1995; Barry and Chorley, 1998).

The differences in the energy fluxes between urban and rural environments are one cause of the UHI phenomenon. Due to atmospheric pollutants, the incoming solar radiation in urban areas is often lower than in rural areas, as part of the radiation is scattered from and absorbed by the particulates. The effect is strongest during low-sun altitudes, when radiation travels a longer distance in the atmosphere. Air quality problems tend to be emphasised during inversion conditions as a result of poor mixing of the lowest air layers (Landsberg, 1981; Oke, 1987). The reduction in short-wave radiation in urban areas is typically less than 10%, but during low wind speed, high relative humidity and cloudless conditions the reduction in global radiation between urban and rural areas can be 25–35 % (Oke, 1987; Erell et al., 2011).

The amount of incident short-wave radiation in urban areas is also affected by albedo. Albedo refers to the proportion of short-wave radiation that is reflected by a surface. The average albedo of the Earth, i.e. the *planetary albedo*, is 0.31 (Barry and Chorley, 1998; Strahler and Strahler, 2006), but there is a large variation in albedo depending on the surface material. Consequently, there are large town-specific differences (e.g. Taha, 1997). It has been estimated that in mid-latitude cities, albedo during snowless conditions is approximately 0.12–0.14, whereas in rural areas it is on average 4% higher

(Landsberg, 1981). During snowy conditions, the difference is often larger, as rural areas are covered with well-reflective snow, whereas the building walls have the same albedo year round. Due to higher temperatures and various slippery-preventive measures, streets in urban areas are often snowless also in winter, partly increasing the urban-rural differences in the albedo. Debris and other dark material in the snow lower the albedo in urban areas and therefore, urban-rural albedo differences exist also between otherwise similar urban and rural surfaces (Oke, 1987).

In addition to the plain material, albedo also depends on 3-dimensional structure. Therefore, an area with erect concrete buildings has an albedo different from that of a flat concrete surface. This is a result of the capture of short-wave radiation that has already reflected from another urban surface. The effect increases with latitude and is accentuated during low-sun seasons. Urban morphology also affects the albedo, as the solar radiation captured by the urban structures increases with the *height-to-width (H/W) ratio*, i.e. the higher the buildings are in relation to the street width, the more radiation is captured. Street orientation also matters, as the albedo is decreased more in east-west-oriented street canyons than in north-south-oriented canyons (Terjung and Louie, 1973; Aida, 1982; Hamilton et al., 2009). As a result of the counteracting effects of the atmosphere and the albedo, the differences in net short-wave radiation between urban and rural areas are small (Oke, 1987; Tsangrassoulis, 2001).

As a consequence of higher urban temperatures, more long-wave radiation is released to the atmosphere compared to the cooler rural surroundings, despite the fact that part of the radiation is trapped into the street canyons (Oke, 1987). The incoming long-wave radiation from the atmosphere is, respectively, increased in urban areas. Thus, similarly to short-wave radiation, the differences in the net long-wave radiation between urban and rural areas are small (Erell et al., 2011).

Despite the small differences in the net short-wave and long-wave radiation between urban and rural areas, diurnal differences in solar heat storage and release are substantial. The thermal capacity and thermal conductivity of urban construction materials are often high compared to those of soils and vegetated surfaces, thus enabling a large amount of solar energy to be stored in the urban structures in daytime. Due to the high-rise urban morphology, the storage surface area is also larger than in more flat rural areas. The stored heat released into the atmosphere during the evening and night is the central factor in the formation of UHI at low latitudes throughout the year and at high latitudes in summer (Oke, 1987; Christen and Vogt, 2004). While the daytime heat storage fluxes in urban areas can be 200 W/m^2, the corresponding rural fluxes are only about one-third of that. Typical night-time heat release fluxes vary between 50 and 80 W/m^2 in urban areas, and between 0 and 30 W/m^2 in rural areas (Cleugh and Oke, 1986; Grimmond and Oke, 1999; Christen and Vogt, 2004).

2.1.2. Anthropogenic heat release

The main sources of anthropogenic heat are heating and cooling of the buildings, depending on the need, vehicle traffic, industrial activity and human metabolism. Compared to the daily average solar radiation, approximated at 450 W/m^2 in the mid latitudes in summer, the amount of energy released by anthropogenic activity is often lower. In winter, however, anthropogenic heat is a crucial component in urban energy balance, often exceeding the impact of solar radiation in UHI formation. In a nutshell, the anthropogenic heat flux density (Q_F) depends on the average energy usage per capita and population density (Oke, 1987; Klysik, 1996; Strahler and Strahler; 2006). Anthropogenic heat can be divided into sensible and latent flow in the air, plus heat in warm waste water. The majority of the methods aimed at quantifying anthropogenic heat release have focused on the sensible heat component, which is often considered equivalent to the energy consumption (Sailor, 2011; Lindberg et al., 2013).

The relative importance of various anthropogenic heat sources is difficult to estimate in general terms, as each town has its own specific characteristics. In general, the role of human metabolism is considered the least important. The Energy Information Association (EIA) reports that in the USA, the building sector consumes approximately 40% of all end-use energy, whereas transportation and industry/manufacturing both account for 30% of the total consumption. In most European countries, the role of the building sector is larger and that of the transportation sector smaller than in the USA (Sailor and Lu, 2004; EIA, 2005; Lindberg et al., 2013). At a city level, the accurate quantification of anthropogenic heating is still a challenge. The methods employed can be divided into inventory approaches, micrometeorologically based energy budget closure methods, and building energy modelling approaches (Sailor, 2011). Of these, the inventory approach has so far been most widely used (Quah and Roth, 2012).

The *inventory methods* are based mostly on energy consumption data, the basic assumption being that the sensible anthropogenic heat release equals the energy consumption. Separating the sensible and latent heat components is not common (see e.g. Klysik, 1996; Ichinose et al., 1999). The accuracy of inventory methods largely depends on the availability and the spatial and temporal resolution of the data. Electricity data are often available only at utility districts or at city level, and traffic data are typically available only for major roads. As a result, a challenge remains in mapping the consumption as a spatially continuous surface. In a fortunate case, electricity consumption and traffic information are available e.g. on an hourly basis, but relatively often the diurnal profiles have to be produced based on annual or monthly data (Sailor, 2011).

The *micrometeorologically based energy budget closure methods* are based on the direct measurements of energy fluxes inside a certain control volume (Oke, 1988). Net radiation can be measured with radiometers, while latent and sensible heat fluxes can

be estimated with eddy covariance techniques. Depending on the timescale, the heat storage component can be ignored or estimated with surface measurements (Mirzaei and Haghighat, 2010; Sailor, 2011). The energy budget closure methods have only been applied occasionally, and with varying success. Measurement errors are a potential pitfall, and the tower used in the flux measurements does not work properly among tall buildings. Consequently, the energy budget closure method is most suitable as a local validator of other measurement methods (Sailor, 2011).

Building energy modelling approaches are generally based on the modelling of energy consumption in the buildings and evaluation of the heat rejection from them. Various environmental loads, such as radiative transfer through windows, are also often included in the models, and latent and sensible heat are separated in the output (Salamanca et al., 2010; Sailor, 2011). A weakness of energy modelling approaches is that they do not include information on any other components of anthropogenic heating. Thus, in order to obtain an inclusive estimate of the anthropogenic heating, building energy models ought to be used in conjunction with an inventory-based approach, including information of the heat release from traffic and buildings that is not incorporated in the building energy model (Sailor, 2011).

Despite these challenges, anthropogenic heat fluxes have been estimated in several studies. Klysik (1996) estimated the average anthropogenic heat flux in the city centre of Łódź, Poland (850,000 inh.) to be 18 W/m^2 in summer and 71 W/m^2 in winter. Summers (1965) estimated the energy flux in Montreal to be 57 W/m^2 in summer and 153 W/m^2 in winter. In Manhattan, New York, the corresponding values were estimated at 53 W/m^2 and 265 W/m^2 (Oke, 1987). Sailor and Lu (2004) studied the energy fluxes of six U.S. cities, namely Atlanta, Chicago, Los Angeles, Philadelphia, Salt Lake City and San Francisco. Averaged over the whole city, in winter, a daytime maximum anthropogenic heat flux of 70–75 W/m^2 was achieved in Chicago, Philadelphia and San Francisco. In summer the corresponding value was 30–60 W/m^2 in most of the cities. Although the averaged anthropogenic heat flux over time and city is mostly under 100 W/m^2, in densely built areas the peak values can be remarkably larger. In the morning rush of central Tokyo, in the middle of the high-rise buildings, a summer maximum anthropogenic flux of 908 W/m^2 has been estimated, and a corresponding winter value of 1590 W/m^2 (Ichinose et al., 1999). As the previously mentioned examples of the mid-latitude cities indicate, the wintertime anthropogenic heat release is generally larger than the corresponding summertime flux, resulting mainly from a larger heating demand during winter. The difference is emphasised in the regions with a cold winter climate (Oke, 1987; Taha, 1997; Wienert and Kuttler, 2005). In low-latitude cities, however, the cooling demand may cause the largest heat release to exist in summer (see e.g. Oke, 1988).

The diurnal variation in the intensity of anthropogenic heat release follows the daily rhythm of human activity, with peak values emerging during morning and afternoon rush hours, approximately at 8 a.m. and 4 p.m. local time. The daytime total heat fluxes are generally higher than the night-time fluxes (Sailor and Lu, 2004). In residential areas, however, night-time heat fluxes from buildings can be larger than during daytime (Quah and Roth, 2012). Sailor and Hart (2006) studied cities located at various latitudes in the United States, and concluded that in summer, the daily variation in total anthropogenic heat flux is rather similar regardless of the climatic zone. In winter, however, the prevailing climate mattered more. Compared to summer, the night-time heat flux was larger due to the increased heating demand. In daytime, the variability in heat flux intensity was smaller than in summer. The relative strength of the morning peak was larger in winter, probably due to lower temperatures and the resulting increase in heating demand (see e.g. Sailor, 2011), whereas in summer the afternoon peak is emphasised as a consequence of the maximum in diurnal cooling demand. Daytime anthropogenic heat release has a weekly rhythm, as the reduced human activity decreases the heat release during weekends (Sailor and Hart, 2006; Sailor, 2011) in the commercial districts of the city. At nights, and in residential areas also during daytime, the anthropogenic heat release may, however, be largest at weekends (see e.g. Quah and Roth, 2012).

To summarise, in daytime in summer, solar radiation can be considered a more remarkable heating agent than anthropogenic heat. During night, however, the role of anthropogenic heat is larger in the urban energy balance. Even though solar radiation ceases at night, its effect appears in the form of heat released from the urban structures, and it may be difficult to distinguish between anthropogenic and solar-based heat fluxes. In high-latitude winter, the role of anthropogenic heat is often more remarkable in UHI formation than that of the energy received from solar radiation (Miara et al., 1987; Fan and Sailor, 2005).

2.1.3. Differences in evapotranspiration

Evapotranspiration is generally lower in urban than in rural areas, resulting mainly from differences in land use; the moisture content of vegetation-covered surfaces is higher than that of the artificial urban surfaces. In addition, plant transpiration also brings moisture to the atmosphere from deeper soil layers. Differences in surface characteristics result in lower absorption of rainwater in urban areas, and the excess water is removed effectively through the sewage or storm water network, this being one reason for the lower urban evapotranspiration. Smaller evapotranspiration in urban areas means more energy in sensible form, thus warming the city environment. (Landsberg, 1981; Oke, 1987; Cotton and Pielke, 1995).

Comparison of urban and rural energy balance reveals that the excess of rural evapotranspiration is largest around midday. In summer, in mid-latitude rural areas, the daytime latent heat flux density is typically 250–300 W/m^2, while in urban areas it remains less than 100 W/m^2. At night, the situation can be reversed, although the differences are negligible. In winter, in rural areas of cold climate regions, seasonal frost, snow cover and plant dormancy effectively diminish evapotranspiration, and in urban areas humidity may be higher also during daytime due to water vapour release into the atmosphere through the combustion processes of traffic and heating (Landsberg, 1981; Oke, 1987).

The Bowen ratio (β) reflects the ratio of sensible heat flux to latent heat flux, i.e.:

$$\beta = Q_H/Q_E \quad (3)$$

In urban areas in very dense and dry districts, β is typically around 5, but in completely built-up city centres the latent heat flux may be totally absent (Oke, 1987; Taha, 1997). Over vegetated surfaces, β is remarkably lower, being on average around 0.5–2. β can also have negative values e.g. at night, when evaporation continues and the latent heat flux is away from the surface, and sensible heat flux is downwards (Oke, 1987). In summer, the daytime sensible heat flux density can be approximately 200–250 W/m^2 in urban areas, and in rural areas about half of that. In urban areas in summer, β stays rather constant throughout the day, but in winter, nocturnal β values of 0.5 can be observed in the city as a result of the moisture content of anthropogenic heating (Christen and Vogt, 2004).

In addition to the urban–rural temperature differences, the effect of evapotranspiration is evident also on an intra-urban scale, as parks are often cooler than built parts of the city (e.g. Upmanis et al., 1998). Increasing the amount of vegetation (green architecture, green roofs) has been utilised as a means to control the adverse effects of high urban temperatures, as more energy is channelled to latent heat through increased evapotranspiration (Gago et al., 2013; Georgescu et al., 2014).

2.2 City-specific features affecting UHI

Although the thermophysical factors shaping the UHI phenomenon are well documented, their combined effects not always are. The spatio-temporal characteristics of the resulting UHI depend on various factors, such as city size, urban morphology, geographical location, topography, proximity of water bodies, and weather. These city-specific features are dealt with in more detail in the following chapters.

2.2.1. City size, urban morphology and geographical location

Oke (1973) observed a positive linear relationship between the logarithm of the city population and the maximum UHI intensity in North American and European settlements.

A UHI of 1 °C can occur in villages with a mere 1000 inhabitants, while maximum UHI intensities of more than 10 °C can exist in cities with a population of a million, the slope of the fitted line being slightly steeper in North American settlements. The correlation between population and UHI is indicative only, especially towards the extreme maxima, as strong UHI intensity reinforces the local wind circulation between urban and rural areas. In practice, this self-organised mixing of air limits the maximum UHI intensity to somewhat above 10 °C (e.g. Bowling and Benson, 1978; Oke, 1987).

In addition to city size, UHI intensity is affected in many ways by the street canyon geometry. UHI is often stronger in cities in which buildings are high compared to the street width. This large *height/width (H/W) ratio* (Oke, 1981) effectively inhibits long-wave radiative loss from the relatively narrow and deep street canyons. Street canyon geometry is a good indicator of population density, and anthropogenic heat release tends to increase with increasing H/W ratio, partly explaining the correlation. High buildings also reduce turbulent heat transport, thus promoting UHI development. Finally, a large H/W ratio often means a high heat storage capacity and, consequently, stronger UHI intensity. However, high H/W ratio can favour daytime UCI due to the thermal inertia of a large building mass plus the shadowing effect of the high buildings (see e.g. Saaroni et al., 2000).

Geographical location naturally governs the overall climate of a city from arctic to tropical settings. Concerning the UHI, the latitudinal location of a city has an effect on solar radiation, evapotranspiration and heating/cooling demand. Wienert and Kuttler (2005) studied the dependence of maximum UHI intensity on latitude by employing data from urban climate studies of altogether 223 cities in the northern and southern hemispheres. They found a positive correlation between the latitude and the UHI intensity, i.e. the highest maximum UHI intensities tend to occur in high-latitude cities. The pattern was explained mainly by differences in anthropogenic heat production and radiation balance. In low latitudes, various measures to mitigate the UHI, such as the carefully designed geometric arrangement of buildings and high albedo of construction materials, may explain some of the latitudinal differences (see e.g. Oke, 1987; Akbari et al., 2012).

2.2.2. Weather

UHI intensity is often negatively correlated with wind speed and cloudiness. In other words, clear and calm conditions are ideal for the development of a strong UHI. Calm weather limits the horizontal mixing of air, thus enabling large urban–rural temperature differences. During cloudless conditions, the radiative cooling in rural areas is often fast, whereas in urban areas, outgoing longwave radiation is partly trapped in the street canyons, and also the heat reserve is larger. Back-radiation from cloud cover effectively diminishes the radiative cooling both in urban and rural areas, thus limiting the probability of large urban–rural temperature differences (e.g. Oke, 1987).

Large weather systems like cyclones and anticyclones, and their impact on UHI have been in the focus of many studies (e.g. Unwin, 1980; Unger, 1996; Morris and Simmonds, 2000; Szegedi and Kircsi, 2003). The effect of synoptic-scale weather on UHI is derived mainly from its effect on wind and cloudiness, and rather often these parameters are used as quantitative means to estimate the connections between the UHI and weather (e.g. Eliasson, 1996; Klysik and Fortuniak, 1999; Magee et al., 1999; Kim and Baik, 2005).

Unwin (1980), Unger (1996), Tumanov et al. (1999) and Morris and Simmonds (2000) have all reported the strongest UHI intensities during anticyclonic conditions, when winds are typically weak and cloudiness is low. In addition to the boosted differences in nocturnal cooling rates between urban and rural areas, during cloudless summer days, solar radiation is stored effectively in urban structures, enhancing UHI development during anticyclonic conditions. In high latitudes, winter temperatures during anticyclonic weather are often relatively cold, provoking heating of buildings and leading to larger anthropogenic heat release. This promotes high UHI intensity during wintertime anticyclones. (see e.g. Klysik and Fortuniak, 1999; Morris et al., 2001; Hinkel et al., 2003).

Compared to cloudiness, wind is often considered a more critical factor in reducing UHI intensity; rather strong UHI intensities may exist during cloudy weather, but with increasing wind speeds, large temperature differences are uncommon (e.g. Ackerman, 1985; Klysik and Fortuniak, 1999; Magee et al., 1999). However, an opposite result suggesting a more crucial role of cloud cover has also been reported (Morris et al., 2001). In summary, the role of cloud cover is somewhat fuzzy compared to wind speed, as also positive correlation between cloud cover and UHI intensity has been reported (Memon and Leung, 2010).

In addition to affecting the UHI intensity, wind speed and direction are known to shape the spatial dimensions of UHI. Klysik and Fortuniak (1999) have observed a multicellular spatial structure of UHI during calm conditions in Łódź, Poland. In addition to the city centre, the housing estates at the outskirts formed independent heat cells, whose temperatures deviated sharply from those of their surroundings. With increasing wind speeds, the UHI formed a single-core structure, with the densest built-up area in the centre. However, in some cases wind is also known to divide the UHI into multiple cells (e.g. Preston-Whyte, 1973). The effect of wind on UHI structure has town-specific variations depending, for example, on the urban morphology and local topography. Regarding wind direction UHI tends to expand with the wind towards the downwind side of the city centre (Klysik and Fortuniak, 1999).

2.2.3. Topography

Topography affects climate on a large spatial scale. In many UHI studies, attempts have been made to eliminate and estimate the impact of topography, as in a few cities only, the relief is so flat that it would not influence spatial temperature differences. One way to offset topographical effects is to use data from sites that are topographically as similar as possible. In some UHI studies, an attempt has been made to eliminate the effect of topography by standardising the temperature observations to the same elevation with the estimated environmental lapse rate. This method has, however, proven problematic, since the atmospheric stratification varies spatially and temporally, and inversions are common, especially at nights (Landsberg, 1981; Goldreich, 1984). Efforts have been made to mitigate the problems connected with the estimation of environmental lapse rate by using regression methods, in which temperatures have been compared against elevation. Additional value is gained only if the correlation proves strong enough. The elimination of topography using regression methods is closely connected to multivariate modelling, in which temperature differences are explained by various environmental factors (Goldreich, 1984). The relative effect of topography on temperature has been estimated with multivariate modelling e.g. by Eliasson and Svensson (2003) and Alcoforado and Andrade (2006).

Based on their topography, Goldreich (1984) categorises cities into four basic types: a. Cities in valleys; b. Cities on slopes; c. Cities on ridges; and d. High-altitude cities. The grouping is indicative only, but it acts as a good framework for comparing the climatic differences of cities in various topographical environments. In the following, the main features of the first three types are discussed with practical examples.

Cities in valleys

Cities located at the bottom of a valley are not as sensitive to night-time inversions as rural valley-bottom areas, since buildings act as mechanical obstacles and prevent or slow down the cold air drainage from the upper slopes. In addition to the mechanical limiting effect of buildings, the heat flux from urban surfaces and the urban canopy layer probably partly prevents the valley-inversions in the urban areas. As a result, especially in the first half of the night, a strong UHI can form between the urban and rural areas located at the valley bottom. A cold katabatic wind can, however, reach the city later in the night, causing a weakening of the UHI, and compared to relatively high hilltop locations, the UHI can change into UCI. Even if the cold air drainage to the urban areas in the valley bottom is blocked, an inversion may develop at a higher level above the valley, and also in these situations, the UHI can prevail only in relation to the low-lying rural places (Kuttler et al., 1996; Bokwa, 2011).

Topography also affects the wind conditions of a city; a valley bottom is sheltered from winds compared to places situated at higher positions. The effect can be observed especially when winds blow perpendicularly towards the valley axis. A valley can, however, act as a wind tunnel and increase the wind speeds when wind blows parallel to the valley axis. Consequently, the indirect effect on UHI depends on the predominant wind direction, and as a rule the sheltering effect favours high UHI intensity via weaker atmospheric mixing (Goldreich, 1984; Bokwa, 2011).

Cities on slopes

The UHI of cities that are built on slopes can be affected by Foehn-type local winds. As the descending air warms dry adiabatically on a leeward slope, the UHI of a city beneath can either weaken or strengthen. If a warm wind blows over a city, it can initiate or strengthen the inversion, thus weakening or dispersing the UHI in relation to an upslope location. If a warm downslope wind reaches the lowest atmosphere only in urban environments that are not so prone to inversions, the temperature difference to the surrounding areas, where the wind keeps aloft, can even reach 20 °C (Nkemdirim et al., 1977; Goldreich, 1984). Goldreich (1984) concludes that apart from the indirect effects of local winds, aspect and slope steepness are rather insignificant topographic factors in urban areas, where their impact is eliminated by the urban morphology. At screen level, the eliminating effect increases with increasing population density and connected higher H/W ratio.

Cities on ridges

Cities located on ridges are not equally well wind-sheltered, but they can still exhibit strong UHI intensities during calm or weak wind conditions, when inversion prevails in surrounding rural areas, thus enhancing the UHI intensity. Goldreich (1971) studied the influence of topography on the temperature differences of Johannesburg (1.3 million inhabitants at the time of the survey) located in the Witwatersrand Ridges in South Africa. The observed temperature differences reached over 10 °C during inversion nights in winter, of which the estimated urban effect was less than half. Laaksonen (1994) studied summer–night UHI in the small settlement of Hyvinkää (ca. 40,000, inhabitants at the time of the survey) in southern Finland, located on top of a hill. Surface inversions developed easily in the surrounding lower-lying rural areas, hence intensifying the UHI. Laaksonen estimated that the topography explained about half of the observed 9 °C temperature difference between the city centre and surrounding countryside.

2.2.4. Water bodies

The high heat capacity of water bodies tends to diminish the diurnal temperature range of adjacent coastal areas in comparison to more continental sites. The proximity of water

bodies also affects the spatio-temporal behaviour of UHI. The strength and character of the effect depend on, for example, the distance from water body, the size and shape of the water body and the temperature difference between the water body and land area, plus wind conditions.

Whether the adjacent water bodies strengthen or weaken UHI intensity depends on the season. Also the spatial pattern of temperatures can be altered. Heino (1978) studied the urban effect on climatic elements in the coastal city of Helsinki (0.5 million inhabitants at the time of the study) in southern Finland. In late autumn and at the beginning of winter, the average urban temperature excess in relation to the more rural inland sites was at its largest as a result of the relatively warm sea. In spring, however, when the sea was relatively cold, the difference in average temperatures was rather negligible, and some inland sites were even warmer than the urban areas. The cooling effect of the sea was most obvious in daily maximum temperatures that were lower in urban than in adjoining rural areas. In each season, the daily minimum temperatures were warmest in the urban areas. The difference was greatest in summer as a result of the joint effect of the sea and the city. Steinecke (1999) studied the local climate of Reykjavik (110,000 inhabitants at the time of the survey), Iceland. In winter, the UHI prevailed the whole day, but similarly to Helsinki, the observed summertime urban cold island was partly explained by the cooling effect of the adjacent sea.

In cities that are located on or near the coast, UHI has an effect on the land–sea breeze circulation. Freitas et al. (2007) modelled the land–sea breeze circulation against the UHI in São Paulo (11 million inhabitants at the time of the survey), Brazil. They found that during daytime, the sea breeze front proceeds firstly to the rural belt between the coast and the city centre located inland approximately 50 km from the coastline. In the afternoon, the daytime UHI with upward air movement creates a local low pressure that is coupled with the low pressure connected with the ascending air at the inland-moving sea breeze front. The coupling speeds up the proceeding of the sea breeze front to the inland, in comparison to the rural areas. The UHI circulation causes the sea breeze front to stagnate over the city, as the winds from inland to the centre of the UHI prevent the proceeding of the sea breeze front. At the same time, the sea breeze front proceeds to the inland in rural areas. Later, the onshore wind ceases the UHI, and the front proceeds further inland passing over the city. At night, the sea breeze turns into a land breeze blowing towards the sea. As the city has its own heat island circulation, the land breeze is affected and may partly be blocked by the UHI circulation in the coastal zone between the city centre and the sea (Freitas et al., 2007; see also Khan and Simpson, 2001).

The role of intra-urban water bodies on thermal comfort has been under discussion by, for example, Saaroni and Ziv (2003). Around midday, the heat stress index, consisting of the combined effect of temperature and humidity, was lower in the vicinity of an urban lake

in Tel Aviv, Israel. The main contributor was a sensible heat loss compared to the sites further away from the lake. In late afternoon and early evening, the lake effect increased heat stress in the adjacent areas. Steeneveld et al. (2014) studied the effect of open water areas on UHI intensity in Rotterdam, The Netherlands, at the end of summer. They found higher daily UHI intensities in sites with more water in their surroundings, as the high heat capacity of water areas keeps them relatively warm during the night. The preceding examples demonstrate that despite the large evaporative potential of water bodies, their usage as a mitigation tool for high urban temperatures is not that straightforward (see also Hathway and Sharples, 2012).

Seasonal ice cover complicates the effect of water bodies on local climate. During ice cover situations, turbulent heat fluxes between water and atmosphere are suppressed. Some heat transfer, however, may take place through the ice and snow via conduction (Brown and Duguay, 2010), although in practice, thick snow-covered ice essentially diminishes the thermal effect of the underlying water. During thick-ice conditions, ice-covered water bodies can be the coldest sites around the city (Fogelberg et al., 1973; Ekholm, 1981). Huovila (1987) has paralleled the microclimate of ice and snow-covered water bodies to the microclimate of an open field.

The relative strength of water bodies as a local climatic factor has been estimated with various modelling settings in a similar manner to that of topography, The variables have been based on the distance from a water body (e.g. Eliasson and Svensson, 2003) or on the areal coverage of a water body (e.g. Unger et al., 2001).

2.3 Modelling of UHI

A large variety of models has been applied to urban climate, and it is challenging to exhaustively categorise them. Atkinson (2003) divided UHI modelling into three approaches: a. Hardware modelling; b. Physical modelling; and c. Dynamical numerical modelling. Hardware model refers to a model that is used to simulate the impact of thermal properties, radiation geometry and surface wetness on surface cooling after sunset. The models are often simplified by eliminating the effect of turbulent heat transfer, as they are meant to reflect calm or weak wind conditions. Under these circumstances, only conduction and radiation are relevant heat transfer mechanisms (Spronken-Smith and Oke, 1999).

Physical models are based on the surface energy budget equation (e.g. Myrup et al., 1993), whereas dynamical numerical modelling also includes, in addition to surface forcing factors, an advective component of the climate (Atkinson, 2003). The urban canopy model is an example of models that are based on energy exchanges between surfaces and air inside a given control volume in the urban canopy. The advanced urban

canopy models include three-dimensional shapes of buildings and separate energy budgets for streets, walls and roofs. Radiative interactions between the streets and walls are also incorporated in urban canopy models. It is possible to include airflow in urban canopy models by defining it as a separate input into the control volume (Souch and Grimmond, 2006; Mirzaei and Haghighat, 2010).

The development of various geographic information systems (GIS) and remote sensing methods and data sets has increased their use in urban climate studies (Svensson et al., 2002; Chapman and Thornes, 2003; Voogt and Oke, 2003; Hart and Sailor, 2009). Instead of using strict numeric energy balance equations, the GIS methods are often based on the estimated thermal characteristics of various land cover forms (e.g. Unger et al., 2011) or urban morphology (e.g. Chen et al., 2012). The quantification is made, for example, by calculating the proportion of impervious surfaces or vegetation cover in a certain area. In addition to land use and urban morphology, other environmental factors, like topography and proximity of water bodies, are also often considered (e.g. Giridharan et al., 2007). It is a challenge for climatology to create a spatially continuous temperature surface from point temperature data. Various interpolation methods have been traditionally used in the spatialisation of temperatures. In an urban environment, temperature can vary sharply within a small area depending on, for example, land use. Therefore, methods that are based only on point information are not able to incorporate factors affecting temperature in the intermediate areas. These 'geometric' or distance-based interpolation algorithms also often lack the ability to satisfactorily extrapolate the information outside the study area. The utilisation of GIS data has enabled more realistic spatialisation of temperatures, as the inclusion of various environmental parameters in UHI modelling has improved the estimation of temperatures to the areas beyond the observation points (see e.g. Szymanowski and Kryza, 2009). Improved availability and spatial coverage of GIS data can be considered a benefit of a GIS-based UHI modelling, especially when the aim is to extrapolate the results beyond the study area.

In UHI modelling, UHI intensity or temperature is commonly the dependent variable, while the choice of explanatory variables depends on the specified focus of the research. Spatially, UHI modelling has been applied with various scales extending from the UHI determined by two observation sites (e.g. Kim and Baik, 2002) to a spatially continuous temperature surface covering the whole study area (e.g. Hart and Sailor, 2009). The spatial scale applied in the quantification of explanatory variables in UHI studies varies too, extending from immediate neighbourhood (Giridharan et al., 2008) to the kilometre scale (Wen et al., 2011).

A broad range of explanatory environmental or weather-based variables has been used in UHI modelling. Variables based on land use, topography and water cover are rather constant in time, unlike dynamic weather parameters. The UHI models applied have

included either environmental or weather-based variables, or both. Only environmental variables are often used when the aim is to estimate the relative strength of those factors on spatial temperature differences. As temperature differences depend partly on the weather, a similar model setting is often run during different weather conditions (e.g. Eliasson and Svensson, 2003; Giridharan and Kolokotroni, 2009). Giridharan et al. (2007) have used wind velocity together with environmental variables in the UHI intensity modelling in Hong Kong. When the interest is principally in the connections between UHI and weather, only weather parameters, such as wind speed, cloudiness and relative humidity, have been included in UHI modelling (e.g. Kim and Baik, 2002). As the urban temperature pattern is dependent on the season and time of day, similarly to weather, specific models are often created for different seasons and day and night. Alternatively, seasonality can also be included in the UHI model (Eliasson, 1996).

The UHI has been modelled with various algorithms. Multiple regression has been used in UHI studies already rather early by, for example, Sundborg (1951) and Lindqvist (1970). Various linear and non-linear regression methods have also been used in later studies (e.g. Eliasson, 1996; Morris et al., 2001; Bottyán and Unger 2003, Yokobori and Ohta 2009; Ganbat et al., 2013). Regression tree methods have been adopted e.g. by Hart and Sailor (2009) and Somers et al. (2013), and geographically weighted regression by Szymanowski and Kryza (2012). Lee et al. (2008) have compared Bayesian entropy mapping and kriging in UHI spatialisation. Gobakis et al. (2011) and Kim and Baik (2002) have used neural network techniques in UHI intensity modelling. The modelling methods applied have often acted as tools to clarify the role of various factors affecting the UHI, although in some cases, the focus has been on the comparison of modelling methods. The variety of the methods applied demonstrates that no single unambiguously best method exists. Rather, the applicability of a given method always depends on the data, the site-specific features and the specified research questions.

3. STUDY AREA

The study area consists of the coastal city of Turku and its surroundings, inside a radius of ca. 15 km from the city centre. During the observation period 2002–2007, Turku had 175,000 inhabitants (2014: 182,000). The total area of Turku is 306 km^2, of which land areas cover 249 km^2. Turku is located in south-western Finland (city centre: 60°27´N, 22°16´E) at the mouth of the River Aura. The Baltic Sea coastline in the region is highly complex with a large archipelago extending towards the south-west of the city (Figures 2a, 2b). This moderates the marine effect in the area. Depending on the large-scale weather systems, either marine or continental air masses can dominate in the area (Arvola, 1987).

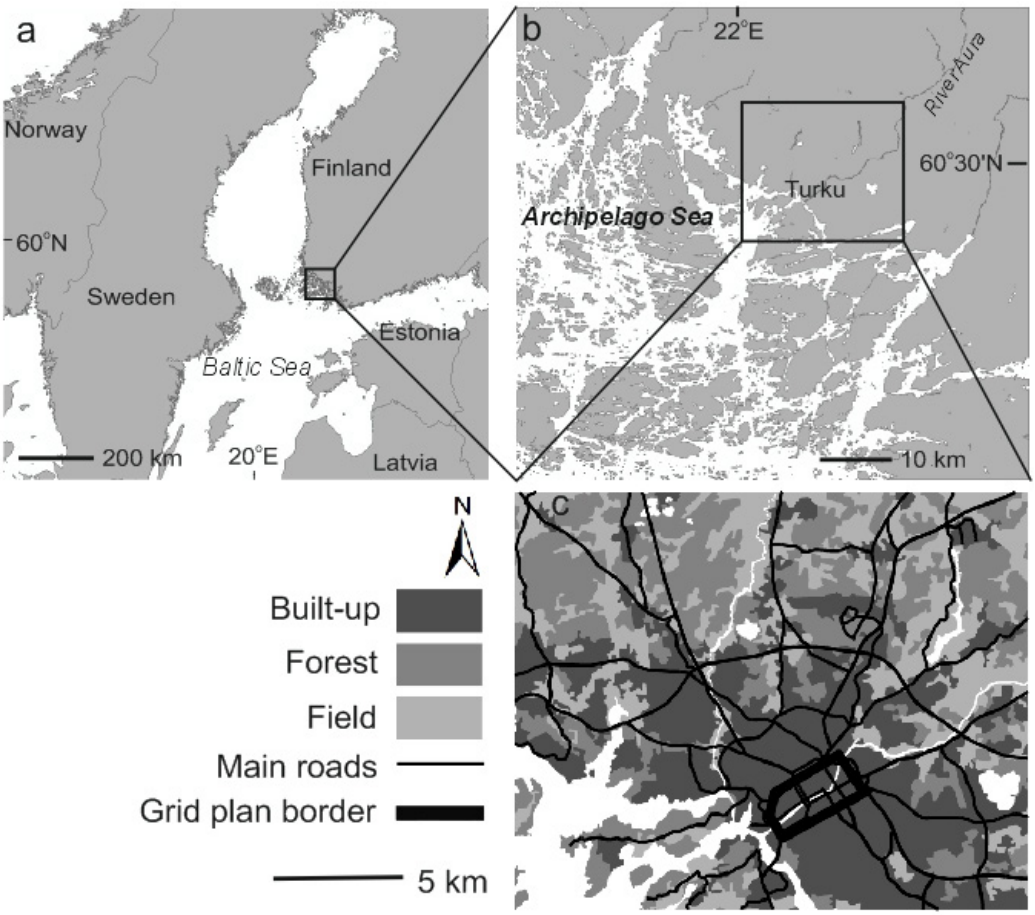

Figure 2. (a) The study area of Turku on the SW coast of Finland. **(b)** The coastline is irregular and the archipelago consists of numerous islands. **(c)** Principal land use, the central road network and approximate border of the grid plan area of the city.

In Köppen's (Peel et al., 2007) climate classification, Turku belongs to the hemiboreal and humid continental Dfb class together with southern parts of the Scandinavian Peninsula, the Baltic countries, and much of Eastern Europe. The same climate type also exists around the Great Lakes Region in the USA and in the Russian Far East around the Amur River basin and northern parts of Sakhalin Island.

The official weather station of Turku with the longest continuous observation period is located at Turku Airport, 7 km to the north of the city centre (Figure 7 and Table 3, site no. 35). The weather station is operated by the Finnish Meteorological Institute (FMI). The annual average temperature for the period 1981–2010 was 5.5 °C. February is typically the coldest month, while July is the warmest, with average temperatures of −5.2 °C and 17.5 °C, respectively (Figure 3). The highest temperature during the 30-year period 1981−2010 was 32.1 °C (2010) and coldest −34.8 °C (1987). Mean annual precipitation is 723 mm, of which 30% falls as snow. The duration of permanent sea ice cover is ca. 3 months starting from the end of December. Ice cover has a remarkable effect on the local climate by limiting the thermal effect of the sea and by effectively making the city more continental compared to iceless circumstances. Due to cyclonic activity, winds are variable in speed and direction (average 3.4 m/s, highest in November, December and January, 3.6 m/s, and lowest in August, 3.1 m/s) (dominant SW with 17% proportion) (Pirinen et al., 2012; Itämeriportaali, 2014; Figure 3). The day length in the area varies seasonally from 6 to 19 hours (Table 1).

Turku city centre is characterised by a grid plan that is approximately rectangular in its form, with a spatial extent of 4 km (SW–NE) times 1.5 km (SE–NW) (Figure 2c). The streets are covered with asphalt or cobblestones and their orientation is from south-west (225°) to north-east (45°) and from south-east (135°) to north-west (315°). The core of the city centre is the market square, located in the middle of the grid plan (Figures 2c, 4). Blocks of flats and parks are the most common land use forms in the grid plan area (**I**: Figure 2). The buildings are mainly 6 to 8-storey stone houses with varying surface colours, ages ranging from late 1800s to the present. Main commercial areas (shopping centres, department stores) surround the market square, while the rest of the built grid-plan area consists mainly of residential buildings.

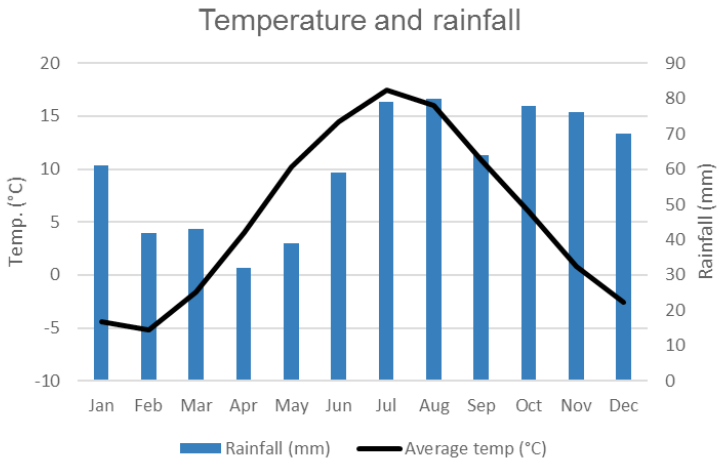

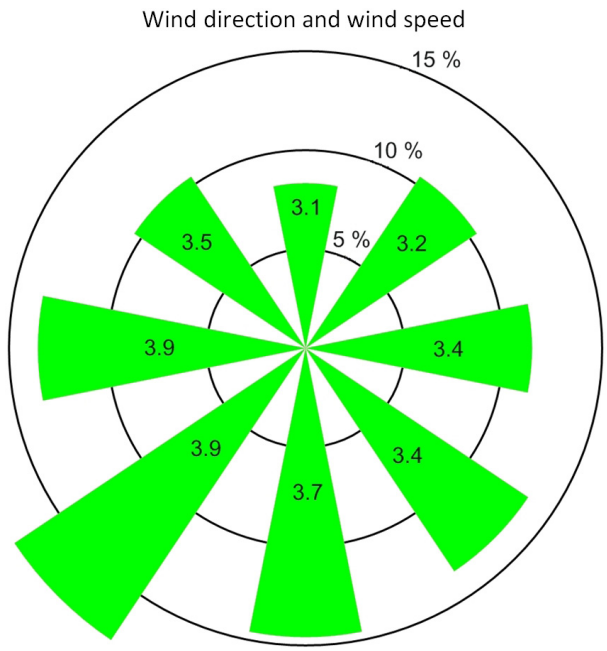

Figure 3. Temperature, rainfall and distribution of wind speed (m/s) and wind direction (8 compass points) at Turku airport in 1981–2010.

Figure 4. An aerial view towards the NE over Turku city centre (Harri Tolvanen, 6.6.2013). The grid plan extends to both sides of the River Aura. The marketplace is marked with the arrow symbol.

The River Aura flows through the grid plan area, where its width varies between 50 and 100 m. The industrial areas lie scattered to the west and north of the city centre, the dockyard and various light industries being the most common branches. Elsewhere outside the grid plan area, the land cover is a mosaic of suburbs, fields and forests. The largest uninhabited and sparsely populated areas are located towards the north of the city centre (Figures 2c, 7). Topographically, the grid plan area consists of flat clay terrain 5–10 metres above sea level, broken through by bedrock outcrops 30–50 m high (Figure 5). The area is old sea bottom, gradually exposed due to post-glacial isostatic rebound during the last millennia. The area still rises ca. 4.5 mm per year (Johansson et al., 2014). Consequently, flat areas consist of marine clay deposits whereas bedrock outcrops have been washed of fine sediments by wave action. Many of the hills around the city centre are partially built on, while some of them host parks in their summit areas. Outside the grid plan, hills alternate with flat areas, and the ground elevation rises gently towards the inland. The highest places of the study area are approximately 70 m above sea level (Figure 5).

Table 1. Day length (hrs:min) and the times (GMT + 2 hrs.) of sunrise and sunset in Turku. Day length varies seasonally between 6 and 19 hours.

	Jan	Feb	Mar	Apr	May	Jun	Jul	Aug	Sep	Oct	Nov	Dec
Sunrise	9:23	8:12	6:49	5:14	3:51	3:02	3:29	4:41	5:57	7:10	8:30	9:32
Sunset	15:58	17:19	18:32	19:49	21:05	22:01	21:43	20:28	18:54	17:23	16:00	15:20
Day length	6:35	9:07	12:43	14:35	17:14	18:59	18:14	15:47	12:57	10:13	7:30	5:48

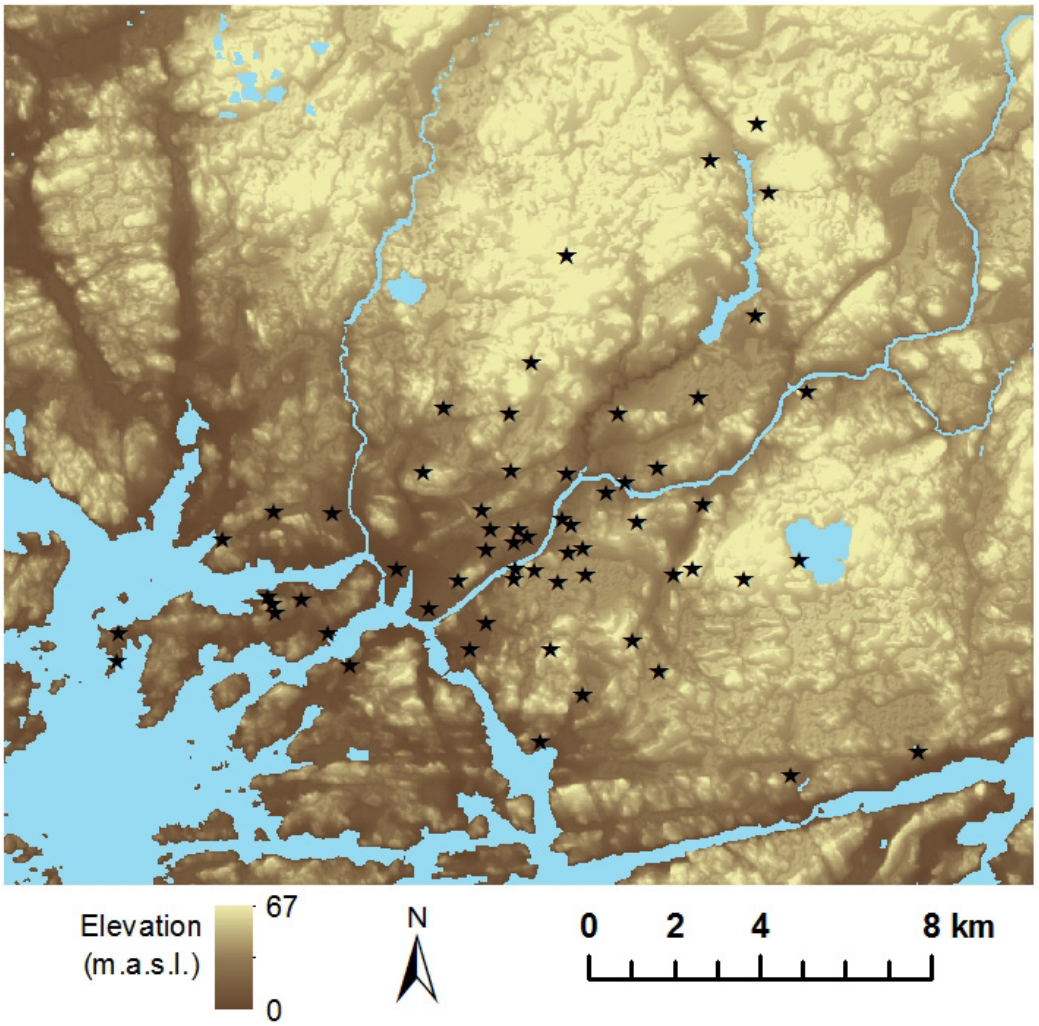

Figure 5. A relief map of the study area based on a national Digital Elevation Model (DEM). The temperature measurement sites are marked with star symbols. m.a.s.l. = metres above sea level.

4. DATA AND METHODS

The temperature and weather data employed in this study were collected by the TURCLIM project (Turku Urban Climate Research Project) maintained by the Department of Geography and Geology at the University of Turku. The data used in the analyses extend from the beginning of 2002 to the end of 2007. Compared to the 30-year period 1981-2010, the six-year period 2002-2007 was 0.4 °C (5.5 °C vs. 5.9 °C) warmer, and the annual rainfall was 40 mm less (723 mm vs. 682 mm). Similarly to the 30-year period, February was the coldest (-5.2 °C) and July the warmest (18.2 °C) month. During the study period 2002-2007, the TURCLIM project maintained altogether 58 Hobo H8 Pro temperature loggers set up to record temperature at 30-min intervals. Since then, the devices have been updated to Hobo Pro U23-001 v2 temperature / relative humidity data loggers (Onset, 2013), and new measurement sites have been established. The accuracy of the Hobo H8 Pro device, as proclaimed by the manufacturer, is ±0.2 °C at 0–50 °C, and the resolution is 0.02 °C. Below 0 °C, the accuracy decreases towards colder temperatures, being approximately ± 0.38 °C at -20 °C. Loggers are placed inside radiation shields on poles at 3 m elevation above the ground (Figure 6). The elevation deviates from the standard 2 m, in order to minimise the risk of mischief in densely populated areas. The TURCLIM observation network is densest in the urban areas, but there are also plenty of measurement sites in various environments enabling meaningful estimation of urban and non-urban effects in the area (Figure 7; Table 3; see also Oke, 2006; Unger et al., 2011). The weather data of the Finnish Meteorological Institute (FMI) have been utilised as a reference in the description of the long-term climatic conditions in the study area. In addition, the cloudiness observations of FMI have been utilised in paper **II**.

Both long-term average temperatures and single observations have been used (Table 2). In the modelling context, the focus has been on long-term averages, as they can be considered more relevant from the city planning perspective, e.g. when the aim is to achieve a more energy efficient city (see e.g. Eliasson and Svensson, 2003). In addition, the integrative aim in papers **I**, **III** and **IV** was to compare the importance of environmental factors affecting the UHI, and with long-term averages the effects of single weather events can be eliminated. The data on shorter periods have been utilised in paper **II**, where the connections between the UHI and weather were studied. The temporal scale of the data extended from momentary situations up to one week.

Figure 6. Hobo H8 Pro temperature loggers. Loggers are placed inside radiation shields on poles at 3 m elevation above the immediate surrounding ground. The site on the photo is in the Varissuo suburb (Figure 7, logger site no. 54).

Table 2. Temperature variables used in the analyses.

Temperature variable	I	II	III	IV
Annual average temp.	x			
Annual average of daily minima	x			
Annual average of daily maxima	x			
Annual average of diurnal temperature range	x			
Monthly average temp.	x		x	x
Monthly average of daily minima	x		x	
Monthly average of daily maxima	x		x	
Monthly average of diurnal temperature range	x		x	
Single observations		x		
Weekly time-averaged temperatures (0.5 hour interval)		x		

In papers **I** and **III**, monthly average temperatures, monthly averages of daily minimum temperatures, daily maximum temperatures and diurnal temperature ranges from years

2002–2007 were used. In paper **I**, annual averages of these variables were also utilised. Only temperature measurement sites with uninterrupted observation periods were included in the analyses, which resulted in the inclusion of 36 sites (Table 4; **I**; **III**). In paper **IV**, the monthly average temperatures in 2006–2007 were used in the analyses. The shorter observation period enabled the use of 50 measurement sites. In paper **II**, four one-week-long case-study periods from the year 2003 were compared, and 58 temperature measurement sites were included in the analyses. The extent of the logger network was ca. 16 km (W–E) x 13 km (N–S) in papers **I**, **III** and **IV**, and ca. 19 km (W–E) x 16 km (N–S) in paper **II**.

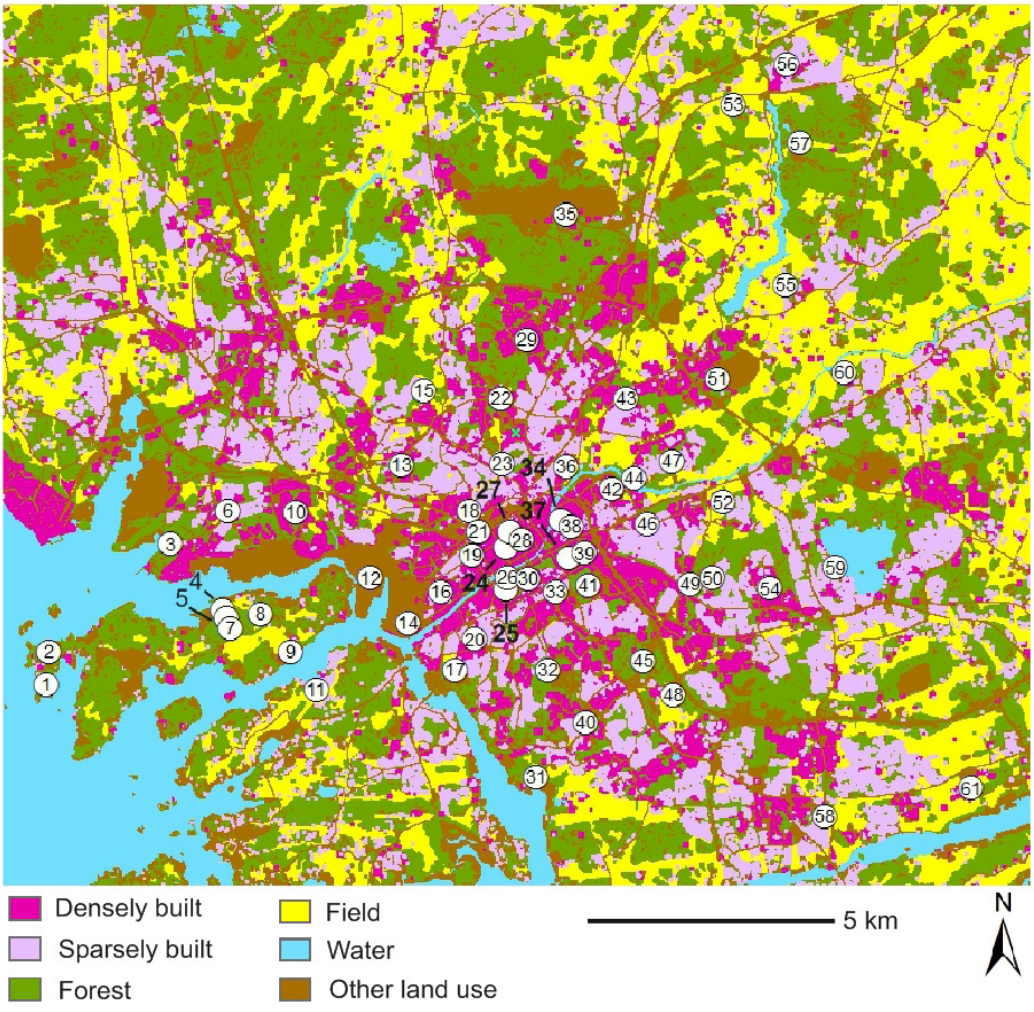

Figure 7. Principal land use forms and the TURCLIM observation sites at the beginning of the study period 2002–2007 based on CORINE land cover data set. Temperature was measured with Hobo H8 Pro temperature logger at each site. At sites no. 28, 49 and 61, other weather parameters were also measured with Vaisala MAWS101 weather stations. Cloudiness observations were made at site no. 35. For more information on the observation sites, see Table 3.

Table 3. Description of the logger sites. Site description is made qualitatively based on the overall characteristics of the measurement site and its surroundings. City centre = marketplace. Land cover information is based on the SLICES land use classification. Two most common (in area) land cover types are identified.

Observation site	Site description	Elevation (m) a.m.s.l	Distance from the city centre (km)	Land cover inside the 100 m radius
1	rural	0.6	10.1	water, forest
2	rural	2.4	9.8	forest, gravel road
3	semi-urban	4.9	7.1	forest, field
4	rural	0.4	6.2	forest, reeds
5	rural	34.7	6.2	forest, gravel road
6	semi-urban	9.3	6.0	gravel field, 2-storey building
7	rural	15.1	6.2	forest, gravel road
8	rural	5.0	5.5	grassland, gravel road
9	rural	1.5	5.2	field, meadow
10	semi-urban	5.8	4.6	parking lot, 2-storey building
11	rural	0.6	5.1	field, forest
12	semi-urban	0.0	3.2	gravel field, high grassland
13	semi-urban	21.2	2.9	forest, block of flats
14	urban	4.6	2.8	grassland, different-sized buildings
15	urban	24.9	3.7	forest, agricultural buildings
16	urban	18.5	1.9	block of flats, gravel field
17	semi-urban	5.8	2.9	forest, asphalt road
18	semi-urban	19.9	1.3	detached house, park
19	urban	10.3	1.0	park, asphalt road
20	semi-urban	10.9	2.2	public buildings, detached houses
21	urban	10.0	0.9	railway, row houses
22	semi-urban	26.2	3.0	parking lot, field
23	semi-urban	30.0	1.7	park, 2-storey building
24	urban	10.6	0.3	blocks of flats, streets
25	semi-urban	25.0	1.0	forest, detached houses
26	urban	7.4	0.7	asphalt road, block of flats
27	urban	27.4	0.4	park, public buildings
28	urban (marketplace)	8.6	0.1	asphalt road, block of flats
29	semi-urban	36.8	4.2	block of flats, 2-storey building
30	urban	30.8	0.7	block of flats, park
31	rural	8.0	4.7	meadow, forest
32	rural	41.2	2.6	forest, landfill
33	semi-urban	20.0	1.2	detached houses, gravel road
34	urban	9.6	0.9	row houses, roads
35	semi-urban (airport)	50.1	6.7	asphalt, grass
35	semi-urban (airport)	50.1	6.7	asphalt, grass
36	semi-urban	19.9	1.8	industrial, asphalt road
37	urban	22.9	1.0	block of flats, asphalt road
38	semi-urban	33.6	1.1	public buildings, asphalt road
39	urban	20.7	1.3	park, asphalt road
40	semi-urban	15.0	3.8	allotment garden houses, forest
41	urban park	20.0	1.6	park, leisure time areas
42	semi-urban	14.8	2.1	detached houses, roads
43	semi-urban	20.1	3.6	public buildings, detached houses
44	rural	0.5	2.6	field, water
45	semi-urban	25.1	3.4	forest, graveyard
46	semi-urban	30.0	2.6	detached houses, roads
47	semi-urban	23.6	3.5	detached houses, forest
48	rural	19.9	4.3	field, roads
49	semi-urban	15.8	3.5	forest, meadow
50	semi-urban	49.9	3.9	block of flats, row house
51	rural	20.0	5.2	landfill, forest
52	rural	12.7	4.2	field, forest
53	rural	34.6	9.9	field, forest
54	semi-urban	45.2	5.1	public buildings, block of flats
55	rural	21.5	7.5	field, forest
56	semi-urban	56.4	11.1	blocks of flats, asphalt road
57	rural	32.4	9.9	forest, meadow
58	semi-urban	16.2	8.2	public buildings, field
59	semi-urban	38.7	6.3	detached houses, lake
60	rural	25.0	7.4	field, forest
61	rural	12.5	10.3	meadow, field

A national Digital Elevation Model (DEM) (NLS, 2009), with a resolution of 25 x 25 m, was used in papers **I**, **III** and **IV**. The SLICES land use classification (SLICES, 2006; **I**; Jaakkola and Helminen, 2002), with a resolution of 10 x 10 m, was used in papers **I**, **III** and **IV**. The floor areas of the buildings were used in papers **III** and **IV**. The DEM and SLICES data cover the whole of Finland, but the floor areas were cost-effectively available only from the Turku municipality area and partly from the Kaarina municipality. The CORINE land cover classification (EEA, 2006) was used in papers **II**, **III** and **IV** in visualising the study area. Although CORINE is a European-wide data set, SLICES was considered better suited for the analyses due to its better spatial resolution and more detailed classification, especially in built-up regions. Landsat ETM+ satellite data were used in paper **IV**. The resolution of the bands utilised in the calculations was 30 x 30 m.

The strength of the urban effect was estimated in this thesis mainly via differences in land use and floor areas of the buildings. SLICES land use classification consists of 45 classes including the following main classes: A = residential and leisure areas; B = business, administrative, and industrial areas; C = supporting activity areas; D = rock and soil extraction areas; E = agricultural land; F = forestry land; G = other land; and H = water areas. In this study, the term land use is meant to reflect both the surface characteristics and the level of human activity affecting the amount of anthropogenic heat release. SLICES classification can be considered detailed enough to meet that aim. Single SLICES classes and their combinations were used as explanatory variables in papers **I**, **III** and **IV**. Due to the high resolution of SLICES and the random spatial matching of the temperature measurement sites and the SLICES pixels in relation to the pixel borders, not only those SLICES pixels that spatially matched the temperature measurement sites were used in surveying the differences in land use between observation points. The broader area was also taken into account because of its effect on temperature. Consequently, the measurement sites represented spatial coverage of a certain land use around them.

In papers **I** and **IV**, the circle-formed buffers of various sizes around the temperature measurement sites formed the footprint area determining the values of explanatory variables. The pixels that spatially matched the temperature measurement sites were naturally also included in the buffer. In paper **III**, the 100 x 100 m resolution grid cells formed the base of calculations, and the cell that spatially matched the temperature measurement site represented it in the modelling context. The hectare grids resulted from summary calculations based on SLICES and floor area data sets. In general, the selected source areas of all of the environmental variables applied were based either on literature, site-specific considerations or statistical estimation of the optimal buffer size.

Table 4. Basic information of the data and methodology of the papers. TURCLIM = Turku Urban Climate Research Project, SLICES = Finnish national land use data set, DEM = Finnish national Digital Elevation Model, FMI = Finnish Meteorological Institute, BRT = Boosted Regression Trees, GLM = Generalised Linear Model, HP = Hierarchical Partitioning.

Paper	Key data sources	Observation sites	Observation period	Key methods
I	TURCLIM, SLICES, DEM	36	2002–2007	Linear regression
II	TURCLIM, FMI	58	2003	Correlation analysis
III	TURCLIM, SLICES, DEM	36	2002–2007	BRT, GLM
IV	TURCLIM, SLICES, DEM	50	2006–2007	HP, linear regression

In earlier studies, different shapes of the footprint areas have been from circular (e.g. by Eliasson and Svensson (2003)) to square (Sakakibara and Matsui (2005)). Temperature measurement sites typically form the centre points of the buffers, but e.g. Costa et al. (2007) have used a buffer with a radius of 350 m to the predominant wind direction and 150 m to the downwind direction. In paper **III**, a square buffer was selected partly because of its better applicability to map the predicted temperatures without overlap or gaps. For land use and floor area variables, the single squares themselves acted as buffers, but in the case of topography and water body, the proper footprint area was considered larger and the buffers were used around 100 m grid cells (cf. Unger et al., 2011). In papers **I** and **IV**, circles with temperature measurement sites as centre points were considered most suitable. Although the distribution of wind directions in the area is uneven, the relevance of the dominance of SW winds is partly diminished by the fact that the wind speed is on average highest when blowing from SW. This causes a better mixing of the air and thus a lower probability of large temperature differences in comparison to the most infrequent northerly winds, which are on average the weakest. (cf. Pirinen et al., 2012). The usage of a symmetrical circle was considered suitable also because urban areas have their own UHI circulation that can deviate from the general wide-scale wind pattern (e.g. Gál and Unger, 2009).

The effect of water bodies has often been assessed in the literature on the basis of the distance to the nearest shoreline (e.g. Eliasson and Svensson, 2003). Since the coastline in the Turku area is highly irregular, and the archipelago to the SW of the city centre extends far to the sea, the distance to the nearest shoreline point was considered somewhat ambiguous. Therefore, the proportion of water surface area around each measurement site was considered a better indicator of the water body effect in the Turku area (**I**; **III**; **IV**).

The range in elevation in the study area is from sea level to less than 70 m. Given the average tropospheric environmental lapse rate of 0.6 °C / 100 m, topography-driven temperature differences during normal atmospheric stratification are small in the area. However, during inversions, the vertical temperature differences are known to be much

larger (e.g. Pike et al., 2013). Thus, the relative elevation of a measurement site was considered more relevant for the temperature differences in the study area than the height above sea level. In addition, the ground elevation rises smoothly towards the inland, and relatively low-lying inland sites could have higher altitude than the relatively high-positioned places near the coast, thus complicating the quantification of the proneness of the places to cold air drainage. The DEM-based relative elevation variables were created by subtracting the average elevation of the measurement site surroundings from the elevation of the logger site (**I**; **III**; **IV**). Of the other topographic variables, the impact of slope steepness and aspect was assessed with the *solar radiation tool* of Arc Map (**I**). As there are no temperature measurement vertical data available in the Turku area, the presence or absence of inversions was estimated based on temperature differences between two or more nearby measurement sites of different elevations, but of otherwise similar environment.

In this study, various modelling methods were used to detect the impact of environmental factors on spatial temperature differences. As linear regression has been widely used in earlier UHI studies (e.g. by Morris et al., 2001; Unger et al., 2001; Kim and Baik, 2002; Bottyán and Unger, 2003; Yokobori and Ohta, 2009; Szymanowski and Kryza, 2009), it was also used here, in papers **I** and **IV**. In paper **III**, a generalised form of linear regression, a *generalised linear model* (GLM), was compared with a novel ensemble method based on machine learning (*boosted regression tree*, BRT), which has been quite a promising analysis and prediction method in different fields of earth and environmental sciences (e.g. Brown et al., 2006; Elith et al., 2008; Hjort and Marmion, 2009). In paper **IV**, the *hierarchical partitioning* (HP) method was used to weed out the strongest urban variable from the group of potential intercorrelated variables. In addition, in paper **IV**, the performance of the urban and other environmental variables was compared with the HP and linear regression.

5. RESULTS AND DISCUSSION

5.1 Temperature variability in space and time

The results presented in papers **I**, **II**, **III** and **IV** indicate that the UHI prevails for most of the time in the Turku area. The densely built city centre in the surroundings of the marketplace is the warmest region in the study area, while the coldest sites are rural inland places slightly over 10 km to the north-east from the city centre (**I**: Figure 7a). This overall spatial temperature pattern is, however, broken on certain occasions, especially in daytime in the spring and in summer, when the semi-urban and rural places often appear the warmest, causing a UCI (Figures 8, 11). On average, the UHI intensity in the Turku area is 1.9 °C, but occasionally the temperature excess of the city centre in relation to the surroundings can be up to 10 °C. The UCI intensity in the area is clearly weaker, being mainly less than 2 °C.

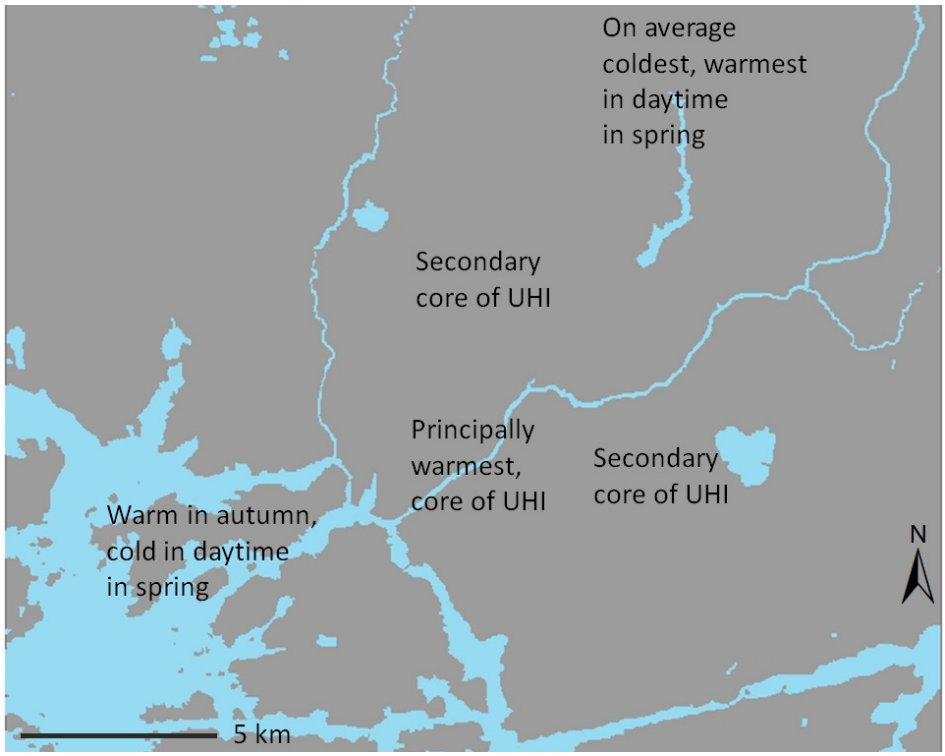

Figure 8. Generalised temperature pattern in the Turku area. The city centre is a principal core of UHI. The suburbs, like Runosmäki and Varissuo (for information on the place names, see Figure 9), form secondary UHI centres. The seasonal variation of sea temperature is seen in the differences in otherwise similar coastal and inland locations.

The temperature variability in the Turku area exhibits both diurnal and seasonal cyclicity, affected by environmental factors and weather conditions. The diurnal and seasonal regularities are observable both in the long-term average temperatures and during short-term study periods. Over the six-year period 2002–2007, the average difference in daily minimum temperatures between the coldest and warmest site was 3.6 °C, whereas the corresponding difference between daily maxima was only 1.0 °C (**I**: Figure 5). Analogous larger variability in long-term daily minimum temperatures than in daily maximum temperatures has been observed by, for example, Wilby (2003) in London in a comparison of two measurement sites. Even if the exact timing of the daily minimum and maximum temperature varies, depending on the measurement site and season, the difference observed in Turku reflects the typical diurnal variation of UHI intensity, with the peak values commonly occurring at night (e.g. Arnfield, 2003; Wienert and Kuttler, 2005). The difference between the ranges of daily minimum and maximum temperatures is largest in summer, reflecting mainly the relatively large impact of solar radiation on the diurnal cycle of spatial temperature differences (**I**: Figure 5).

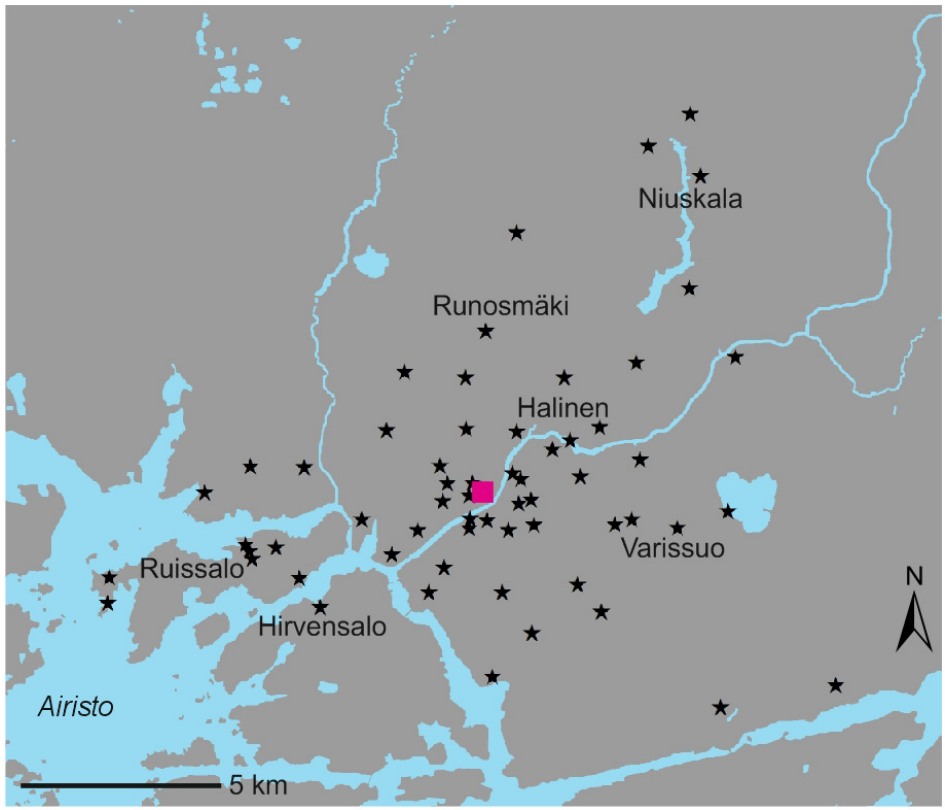

Figure 9. The study area with place names mentioned in the text. The square in the city centre denotes the marketplace, and stars the other logger sites (n=61).

The UHI intensity in Turku is affected by weather conditions in that it correlates negatively with wind speed and cloudiness. Wind speed seems to be the more critical factor of the two in suppressing UHI intensity. When wind speed exceeded 3 m/s, UHI intensities of more than 2 °C were not observed, while UHIs of approximately 6 °C were still detected with the total cloudiness of 6/8 (**II**: Figures 11c, 11d). In accordance with the conclusions of Klysik and Fortuniak (1999) concerning the UHI of Łódź, Poland, only overcast conditions seem to eliminate the strong UHIs in the Turku area.

Although the city centre is typically the core of the UHI in Turku, suburbs like Runosmäki and Varissuo (Figure 9) form secondary UHI centres (Figure 8), especially under calm and cloudless weather. The land use pattern in the Turku area favours a multicellular UHI, as there are many densely built high-rise suburbs in 3–5 kilometres distance from the city centre, and rather sparsely built or detached house areas in the intermediate zone. With higher wind speed and cloudiness, separate suburban UHIs are not present, but UHI often has a single-core structure with the city centre as the core. Analogous weather-dependent dichotomy in the UHI structure has been observed, for example, by Klysik and Fortuniak (1999) in Łódź, Poland.

In the long-term monthly temperatures, there are two seasonally noteworthy features. The spatial temperature variation is larger in summer than during other seasons. This pattern is most obvious in daily minimum temperatures, but detectable also in average temperatures and daily maxima. In daily minimum temperatures, the difference between the warmest and coldest site was largest, 4.8 °C, in August, whereas the corresponding difference was at its lowest, 2.3 °C, in November (**I**: Figure 5). Similar larger variability in daily minimum temperatures in summer has been observed also by e.g. Ackerman (1985) in Chicago and Wilby (2003) in London. In these studies, only a few measurement sites were compared to reflect the diurnal and seasonal variation in UHI intensity. In Turku, 36 sites were included in the comparison, but the observed differences can be considered to rather well reflect the seasonal variation in night-time UHI intensity, as the average minima were typically highest in the marketplace and lowest in the rural site Niuskala (Figures 9, 7 and Table 3, site no. 57).

The existence of the largest temperature differences in the Turku area at the end of summer demonstrates the combined effect of environmental and radiative factors. In August, the daytime solar heat storage is still substantial. Nights are longer than in the middle of the summer, increasing the probability of stable atmospheric stratification. In urban areas, the inversion sensitivity is lowered by the heat release from buildings and horizontal surfaces (e.g. Bornstein, 1968). In particular the role of horizontal urban surfaces as a heat source is large compared to the seasons with lower insolation. The differences in inversion sensitivity between the urban and rural areas are supposed to be largest in the region at the end of summer, this being one reason for the existence of the

largest minimum temperature differences in that season. The water bodies in the Turku area are relatively warm at the end of summer, promoting the night-time temperature excess of the coastal and urban areas compared to the inland sites (**I**; **IV**).

The occurrence of the smallest minimum temperature differences in November can be explained by the seasonal cycles of solar radiation and anthropogenic heat release. Solar radiation in November is a rather insignificant factor compared to the summer months. The heating season has started, but the temperatures are milder than in the middle of the winter. Consequently, the anthropogenic heat release originated from the heating of the buildings is lower than in the winter months (e.g. Hinkel et al., 2003). As a result, the rather low combined effect of solar and anthropogenic heating can be considered as principal reason for relatively small temperature differences at the end of autumn.

Another seasonal regularity is the shift of the relatively warm areas, driven by the sea temperature. In the autumn, when the sea temperature is relatively high, coastal places are the warmest superseded only by the city centre (Figures 8, 10). A reversal takes place in daytime in the spring, when coastal places are the coldest and rural inland places the warmest, reflecting the effect of a relatively cold sea (Figure 8; **I**: Figure 7c). The daytime UCI that is also observed in summer (**II**: Figure 15) can be considered an indicator of the propagation of the sea breeze front in the Turku area. The irregular widespread archipelago partly complicates the sea and land breeze circulation in the area, but the lower daytime temperature in the city centre compared to the inland indicates that the average position of the maximum propagation of the front would be somewhere between the city centre and the observation sites furthest inland (cf. Freitas et al., 2007).

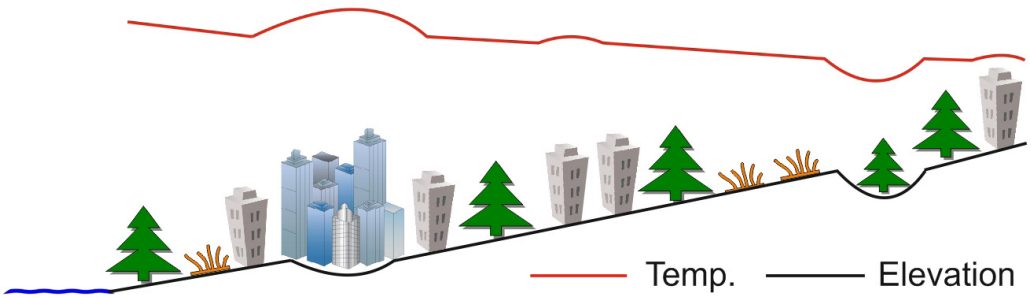

Figure 10. Generalised temperature profile in autumn. The city centre is the warmest, followed by the coastal zone. Suburbs form secondary heat islands. Rural valleys are more prone to cold air drainage than urban valleys.

The larger and more regular diurnal cycle of UHI intensity in summer, with the daytime UCI, was also apparent on a shorter timescale, resolved in the comparison of two one-week-long summer and winter periods (**II**). The summertime UHI reached its maximum

intensity 2-4 hours after sunset. During clear and windless conditions the time-averaged maximum UHI intensity was around 6 °C, but during single nights, the intensity grew to up to 8 °C. The UHI intensity remained rather constant even up to two hours after sunrise, when it started to weaken. The UHI turned into UCI about two hours before noon. The time-averaged UCI intensity was less than 1 °C, but during single days it reached the intensity of 2 °C. With higher wind speeds and cloudier conditions the summertime UHI was weaker, with the average maximum intensity of approximately 4 °C. The UHI also started to weaken earlier at night during the cloudier and windier study period (**II**: Figures 16, 17c, 17d, 18c, 18d). The dynamic pattern is analogous to the UHI intensity curve differences observed by Oke and Maxwell (1975) in Montreal between two slightly different summer night conditions, albeit the UHI intensities in Montreal were in both cases larger. Compared to the results of Oke and Maxwell (1975) in Montreal, Wilby (2003) in London and Charabi and Bakhit (2011) in Muscat, Oman, the summer night maximum UHI intensity in Turku was reached earlier at night. This is probably due to larger heat storage capacity in Montreal, London and Muscat, which are larger and located at lower latitudes than Turku. Oke and Maxwell (1975) also studied the UHI rhythm of Vancouver, which is closer to Turku both in size and in latitude, and the timing of the maximum UHI intensity matched that of Turku rather well, albeit the UHI intensity level was higher in Vancouver. In summary, the differences between the summertime study periods concerning the connections between the night-time UHI intensity and weather are in agreement with earlier studies (e.g. Tumanov et al., 1999; Kolokotroni and Giridharan, 2008) indicating higher UHI intensity during calm and clear conditions.

In Turku, the timing and intensity of UCI also depended on the weather. The morning shift to the UCI happened later during windier and cloudier weather, and the UCI intensity was weaker than during calm and clear conditions. The observed connections between the daytime UCI intensity and weather are supported, for example, by the observations of Svensson and Eliasson (2002) in Gothenburg. They found stronger UCI intensity during clear and weak wind conditions, although their data also included winter months. The difference in Turku can be explained by larger differences in thermal inertia between urban and rural sites during a calm and clear study period, when the temperature rise is faster in the morning compared to other study periods. In addition, the generally weak wind promotes the local sea–land breeze circulation that can also explain the larger temperature difference between the city centre and the rural inland place Niuskala (Figure 9; Steinecke, 1999).

In winter, as expressed in time-averaged values, the UHI prevailed throughout the day. This observation is in agreement with that of Steinecke (1999) in Reykjavik, Iceland. During the clear and windless study period, the time-averaged UHI intensity in Turku

was around 4 °C during the 18 hours when the sun was below the horizon. During daytime, the intensity weakened to 2–3 °C. During the cloudy and windy study period, the UHI intensity varied mainly around 1 °C throughout the day, and the variation in intensity reflected weather events more than the time of day. During both of the winter study periods, the maximum in UHI intensity was detected 5–7 hours after sunset despite the dominance of weather events affecting the UHI intensity (**II**; Figures 16, 17a, 17b, 18a, 18b). The timing of the maximum UHI intensity matches quite well with Oke and Maxwell's (1975) winter observations during calm and clear conditions in Montreal. During cloudier and windier conditions, the saturation of UHI intensity curve emerged earlier in Montreal than in Turku. As the diurnal amplitude in the UHI intensity is clearly smaller in winter, the observed differences in the times of the peak UHIs between Turku and Montreal can probably be explained by factors other than city-specific differences.

In winter, the UHI has a secondary high intensity phase in the morning, reflecting heat release by traffic after the night hours with little human activity (**II**: Figures 16, 17a, 17b; cf. Sailor and Lu, 2004). Even if there is a weak diurnal rhythm detectable in the time-averaged winter UHI, especially during calm and windless conditions, the daily comparison indicates that during winter, the daily minimum UHI can exist either during daytime or at night, and the UHI intensity can stay constant and strong throughout the day. In summer, exceptions from the average daily UHI rhythm were more infrequent, albeit, for example, due to local rain showers, the maximum UHI intensity emerged in the afternoon instead of night. Although, on average, the UHI prevailed in winter throughout the day, the daily comparison revealed a momentary night-time UCI (**II**: Figure 18b), which is also a good indicator of the randomness in the diurnal UHI intensity cycle in winter.

The largest single temperature difference, 10 °C, was measured in winter, although the long-term spatial temperature differences were largest at the end of summer, and the night-time UHI intensities were generally stronger during summer than during the winter study periods. The maximum difference occurred during the calm and clear study period in January at 0:30, when the temperature in the inner court of a housing quarter in the city centre approximately 350 m to the SW of the marketplace (Figure 7 and Table 3, site no. 24) was – 18.5 °C. Simultaneously, a temperature of – 28.5 °C was measured approximately 3 km NE of the city centre, in a relatively low-lying rural patch beside the dam and rapid of the River Aura (Figure 7 and Table 3, site no. 44; **II**: Table 3, Figure 14a). The large temperature difference was a result of calm weather and a large anthropogenic heat flux in the city centre due to the high heating demand induced by low temperatures (cf. Lindberg et al., 2013). In addition, an inversion prevailed in rural areas and also in the city centre. Analogously to Turku, Klysik and Fortuniak (1999) conclude that in Łódź, Poland, favourable conditions for a strong UHI exist most often in summer,

but they observed the strongest single UHI ever recorded in Łódź in their case study carried out in February. In Volos, Greece, Papanastasiou and Kittas (2012) found the average maximum UHI intensities to be of similar magnitude in summer and in winter, but the highest single UHI values occurred in winter. Magee et al. (1999), in their urban climate study in Fairbanks, Alaska, recorded the highest UHI intensities in winter, both in average and absolute terms.

Beyond the cold and calm winter study period, the next largest momentary temperature differences occurred in summer. During the calm and clear study period at 1:30 at night, an 8.4 °C UHI was recorded, while during the cloudier and windier study period, a 7 °C UHI was observed at 21:00 in the evening. During the cloudy and windy winter study period, the largest single temperature difference was 4.6 °C, measured at 22:30. Each of the maximum divergence moments were UHI situations, as the city centre was the warmest site. The sites that were coldest in the long-term were not the same ones that were momentarily the coldest. The latter were located closer to the city centre, within 3–5 kilometres distance (**II**: Table 3, Figure 14b, 14c, 14d). These sites are rural patches surrounded at least from two cardinal directions by semi-densely built residential areas. The relatively low-lying and uninhabited coastal site of Hirvensalo island (Figure 9) was the coldest site during the largest momentary temperature differences, both during the calm and clear summer, and the windy and cloudy winter study periods (**II**: Figures 14b, 14d). This site was also the coldest in average terms at the beginning of the night during the calm and clear summer study period, being, as in the extreme situation of wintertime, a good indication of the existence of rather sharp small-scale temperature variability during favourable weather conditions (cf. Klysik and Fortuniak, 1999; Szymanowski and Kryza, 2009). Considering the summertime UHI dynamics, the location of the coldest site was to the south-west of the city centre only during the calm and clear study period early in the night. This is probably due to the stronger land–sea breeze in calm and clear weather. In the evening, the land breeze together with the UHI circulation slows down the development of inversions in the regions inland from the city centre, whereas the places to the south-west of the city centre are partly blocked from the effect of land breeze (Freitas et al., 2007). A similar shift was not observed during the cloudier and windier summer study period, when the coldest site already early in the night was the northern rural site Niuskala (Figure 9).

In general, the largest summer and wintertime temperature differences in Turku seem to exist at night during calm or weak wind conditions. The link to cloudiness is not equally well defined. The timing of the cloud observations at three-hour intervals did not match exactly the maximum divergences. Regarding the largest temperature difference in winter, the cloudiness 1.5 hours before the UHI peak was 1 octas, and 1.5 hours after the peak 7 octas. In summer, the preceding cloudiness observation 2.5 hours before the

extreme temperature difference and the next observation half an hour after the extreme were both 1 octa, suggesting the possibility of a larger significance of cloud cover in summer than in winter, a phenomenon that has been observed by, for example, Ganbat et al. (2013) in Ulan Bator, Mongolia.

In Turku, the largest summer and wintertime temperature differences observed were caused by a strong impact from the UHI drivers typical of those seasons, i.e. solar radiation and anthropogenic heat release, respectively. During the preceding day, before the summertime maximum, the cloudiness was 1 octa throughout the day, enabling unrestrained solar heat storage. In addition, at the time of the maximum divergence, the inversion prevailed apart from in the city centre. During wintertime maximum divergence, the cold weather resulted in a higher-than-average anthropogenic heat release, and promoted the strong UHI. During summer and winter, the inversions also affected the UHI development. Compared to the long-time average temperatures, the impact of topography seems to be emphasised during weather conditions favourable for inversions. Due to the heat release from the urban canopy layer, the effect tends to mainly strengthen the UHI intensity. A similar connection between the UHI intensity and atmospheric stratification has been observed by e.g. Magee et al. (1999) in Fairbanks, Alaska, and He et al. (2013) in Changsha, China.

5.2 Temperature modelling

Various modelling methods were employed to estimate the impact of land use, topography and water bodies on the spatial temperature differences. The modelling was applied mainly to the monthly average temperatures (**I**; **III**; **IV**), but also to the averages of daily minima, maxima and diurnal temperature range (**I**; **III**). In paper **I**, the temperatures of the whole 6-year (2002–2007) observation period were also modelled.

The environmental variables succeeded rather well in explaining the observed temperature differences in the Turku area. In a linear regression model that was calibrated for each month and the whole observation period, the explanatory power of average temperature, daily minimum temperature and diurnal temperature range models was in general higher than the explanatory power of the daily maximum model (**I**). In the methodological comparison of BRT and GLM, the diurnal superiority of the models was not as clear, even though the model calibration succeeded most seldom in daily maximum temperatures and also the model evaluation results were in general poorest with the daily maxima (**III**). The results concerning the better performance of the minimum temperature models compared to the maximum temperature models are in line with the observations of e.g. Eliasson and Svensson (2003) in Gothenburg and Kolokotroni and Giridharan (2008) in London. They obtained higher R^2 values in night-time than in daytime regression models.

The linear regression model was calibrated for average temperatures with two slightly differing modelling settings (**I**; **IV**). In both of them, the explanatory power of the model was best in March. In both cases, the effect of sea areas was so minimal that the variable was not included in the model. In contrast, the effect of relative elevation was at its strongest, reflecting higher temperatures at higher positions. The existence of the highest explanatory power in spring may result from the better emergence of the city effect and of relative elevation, as the effect of water bodies is rather neutral. The performance of relative elevation is improved by the early spring conditions that favour inversions; even if the air masses gradually warm when the spring proceeds, the snow cover keeps the lowest air layers relatively cold. The presumption is also supported by the highest explanatory power of the only daily minimum temperature model that was calibrated for each month (**I**: Table 5b). Both the explanatory power of the model and the relative role of topography were largest in March, as in both average temperature models. The directions of the effects were also similar, indicating higher temperatures at higher positions. The best model performance of monthly-based maximum temperatures existed in April (**I**: Table 5c), which is explained mainly by the strong cooling impact of water bodies. The observed highest explanatory powers of monthly average and minimum temperatures in March and daily maximum temperatures in April are parallel with the seasonal comparison by Eliasson and Svensson (2003), as they also obtained the highest single daytime and night-time R^2 values in spring in their multiple regression models.

In temperature modelling, the explanatory variables were constructed by taking into account the surroundings of the temperature measurement site. The size and shape of the 'circle of influence' or 'footprint area' varied depending on the variable and the modelling setting, and the selection was based on earlier studies, site-specific features (**I**; **III**) or statistically determined optimal buffer sizes (**IV**). The results of the statistically determined optimal buffer sizes showed that the optimal source area for urban variables was either 300 m or 1000 m (**IV**: Table 4). The values fit inside the scale that has been applied in earlier UHI studies (e.g. Giridharan et al., 2008, Wen et al., 2011). In addition, it is in line with Oke's (2006) estimation of 0.5 km as an approximate circle of influence area in screen level temperature measurements. For non-urban variables, the variation was larger, as the optimal buffer size extended from 100 m to 20000 m. Compared to the urban variables, the mode and average of the determined buffer sizes were larger. The observation is consistent with Giridharan and Kolokotroni's (2009) and Stewart and Oke's (2009) considerations of the appropriateness of a larger buffer size in a more sparsely built or natural environment.

Seasonally, the optimal buffer size of the urban variables was largest in spring and smallest in autumn and winter (**IV**: Table 4). The seasonal pattern is in line with the opinion of Giridharan and Kolokotroni (2009), who conclude that in summer, the source

area for urban variables should be larger than in winter. For non-urban variables, the buffer size was on average largest in summer and smallest in spring. The seasonal variation in optimal buffer sizes was more homogeneous among urban variables than among non-urban variables, the latter including variables that had totally opposite seasonal patterns. Consequently, the site-specific features and their seasonal impacts can be considered even more relevant in the selection of buffer zones for non-urban than for urban variables. In general, the variable-specific and seasonal variations in determined optimal buffer sizes indicate that the performance of the model could be improved by buffer size testing before the analyses. Depending on the testing and modelling methods, the variables can, however, behave differently as part of a model and in preliminary evaluations. Therefore, site-specific considerations and earlier experience of the applied buffer size can also be considered justifiable ways to select the footprint area.

Methodologically, the explanatory power of linear regression models varied depending on the season, time of the day and applied variables. The modelling settings deviated from those of BRT and GLM, and the results are not directly comparable. In the comparison between BRT and GLM, identical variables were compared, and GLM was in general more appropriate in the model settings at issue (**III**: Tables 2, 3). The BRT model has earlier been observed to reach its optimum prediction ability at a rather large number of observations, i.e. 100–200 (Hjort and Marmion, 2008). In addition, the employed variables and their buffer sizes can have an effect on the performance of a model (Luoto and Hjort, 2006, Hjort et al., 2010). Consequently, the applicability of the BRT method in the UHI context is worth further studies.

Like the BRT, HP is another new method in the UHI context. In the UHI modelling settings, a large variety of urban variables has been applied. As the variables often reflect rather similar thermophysical impacts and processes, the problem of intercorrelation between the explanatory variables is common (e.g. Giridharan et al., 2007). Consequently, only one or few potential urban variables can often be meaningfully included in a given model. Naturally, the multicollinearity problem may actualise also among non-urban or weather-based variables (see e.g. Nkemdirim, 1980). In paper **IV**, the HP method was used to sift from the group of potential explanatory variables the urban variable that had the most independent effect on temperatures. Thereafter, the independent effect of the strongest urban variable was compared with the non-urban environmental variables using HP and the linear regression model. Both methods highlighted the importance of the urban variable on spatial temperature differences. The relative importance of the non-urban variables had slight differences depending on the method, but in general, the results are in harmony. Even if the variable does not necessarily behave in a same manner as a part of a multivariate model as in HP, the method is a noteworthy option to ease the selection of intercorrelated environmental variables to be included in the

model. The applicability of the method could be concretised e.g. when considering optimal reclassification of a detailed land use classification based on thermal properties of the original land use classes. The inability of HP to assess non-linear relationships is, however, a weakness of the method (Hjort and Luoto, 2009).

5.3 Effects of environmental factors

The modelling results demonstrate a seasonally and diurnally varying pattern in the explanatory power of urban and other environmental factors (**I**; **III**; **IV**). In general, for minimum and average temperatures, the urban land use has a warming impact throughout the year. The effect of water bodies is twofold: a cooling impact is seen in the springtime daily maximum temperatures, which are lowest near the coast and highest inland. In autumn, the relatively warm sea heats the coastal areas. The impact of topography materialises in the vulnerability of low places to cold air drainage during night-time (Table 5). Below, the effects of environmental factors are assessed by dividing them into the impacts of water bodies, topography and land use.

Table 5. The direction of the effect of the most crucial environmental factors on temperatures (+ = warming, - = cooling)

Urban land use	**Winter**	**Spring**	**Summer**	**Autumn**
Average temperature	+	+	+	+
Daily minimum temperature	+	+	+	+
Daily maximum temperature	+	+	+	+
Diurnal temperature range	-	-	-	-
Relative elevation				
Average temperature		+		
Daily minimum temperature	+	+	+	+
Daily maximum temperature				-
Diurnal temperature range	-	-	-	-
Water bodies				
Average temperature	+	-	+	+
Daily minimum temperature	+	+	+	+
Daily maximum temperature	+	-	-	+
Diurnal temperature range	-	-	-	-

5.3.1. Water bodies

The coastal location of Turku complicates the detection of the urban effect on the spatial temperature differences in the area. The influence of the Baltic Sea occasionally extends to the city centre although the wide archipelago zone buffers the marine impact. The River Aura and the few lakes in the region also impact the local climate, but compared

to the sea, their effect is minute and local. Compared to other environmental factors, water bodies have a more distinct seasonal character both in the relative strength and the direction of the effect.

In the autumn and early winter, coastal areas are relatively warm due to the warming effect of the sea. The impact is manifested, for example, in the western part of Ruissalo island facing Airisto, the largest open water area in the region (Figure 9). The heating effect is strongest in October and November. In November, the difference in average temperatures as well as daily minimum and maximum temperatures between the city centre and the camping site in the western parts of Ruissalo island was only 0.2 °C, the camping site being the second warmest site immediately after the marketplace located in the city centre (**I**). The sea-facing regions in Ruissalo form secondary heat island centres, similar to suburbs, as there are colder regions between them and the city centre. The fact that the UHI core remains in the city centre suggests that urban land use is a stronger warming agent than the sea also in the autumn and early winter. The modelling results, however, demonstrate that whether it is the water bodies or the urban variable that dominate depends on the circle of influence applied, and on the modelling method. For example, the linear regression models (**I**: Table 5a; **IV**: Table 7) produced slightly different results concerning the importance of water bodies on average temperatures. In paper **I**, the urban land use is the strongest variable throughout the year, albeit the impact of water bodies is almost as large in autumn. In the linear regression carried out with optimal buffer sizes (**IV**), the water body variable was the most important variable from October to January, the effect being warming in each month. In the GLM model, the contributions of water bodies and urban land use were equal, while in the BRT, the sea impact dominated (**III**: Table 2). Concerning the daily minimum temperatures, the GLM and BRT methods highlighted the impact of water bodies, whereas in linear regression, the urban land use outperformed the water body variable also in autumn (**I**: Table 5b; **III**: Table 2). The heating impact of the sea is also seen in daily maximum temperatures in the autumn and early winter, albeit the urban land use outperforms the water body variable except for November, when the water body variable is the strongest (**I**: Table 5c). Altogether, the results concerning the dominance of either water bodies or urban areas in the generation of the differences in average as well as daily minimum and maximum temperatures in autumn were contradictory. Hence, the effects can be concluded to be somewhat equal.

The heating impact of water bodies weakens during winter. In spring and during the first half of summer, the impact on average temperatures is negligible (**I**: Table 5a; **IV**: Table 7). As for minimum temperatures, the effect is slightly warming (**I**: Table 5b), whereas for daily maximum temperatures, the impact has reversed to a clear cooling effect in the spring (**I**: Table 5c; **III**: Table 2). Both modelled and measured temperatures demonstrate that the cooling impact of water peaks in April and May: the daily maximum

temperatures in the western tip of Ruissalo island are on average 1.6 °C colder than in the rural inland place Niuskala (Figure 9; **I**: Table 5c, Figure 7c). The cooling impact extends from March to August. Compared to other environmental factors, the relative role of water bodies is emphasised in linear regression. In maximum temperature models from April to June, water body was the only variable included in the model (**I**: Table 5c). In GLM, water body was the strongest variable, but in BRT, the heating impact of urban variables outperformed the cooling impact of water bodies (**III**: Table 2).

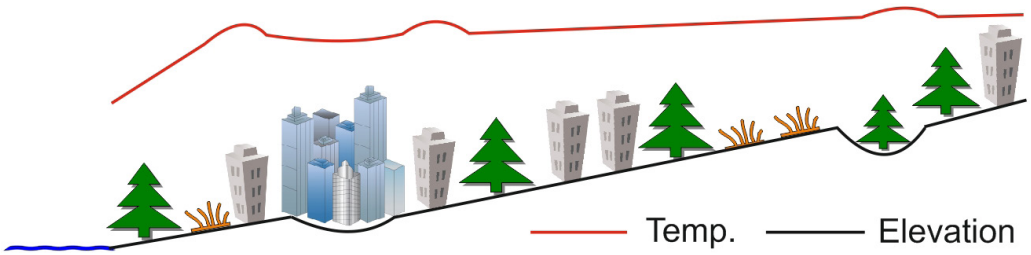

Figure 11. Generalised daytime temperature profile in spring and summer. A moderate UCI exists. The suburbs and topographically favourable inland sites are the warmest. The coastal zone is the coldest.

In spring, an urban cold island evolves in the city centre, in comparison to the more rural inland location (**I**: Figure 5c). A probable reason for the UCI is the propagation of a sea breeze front that extends to the city centre. During the summer study periods, a morning UCI formed not only in relation to inland location, but also in relation to equally sea-affected places in the neighbourhood (Figure 11; **II**: Figure 15). This suggests that it is not only the maritime effect that creates the UCI in the study area, but the building mass and the shadowing effect of the buildings cause enough thermal inertia to affect the UCI structure in the morning.

5.3.2. Topography

Compared to land use and water bodies, the effect of topography proved to be weaker in explaining the differences in monthly (**I**; **III**; **IV**) and annual temperatures (**I**). Momentarily, however, especially during inversions, the impact is emphasised (**II**).

The effects of slope steepness and aspect on temperatures were negligible, correlating positively, but not significantly, with temperatures (**I**: Table 4). The observation is in agreement with those of Goldreich (1969; 1971) in Johannesburg. The mosaic of vertical and horizontal surfaces in the city probably suppresses the impact of slope direction and gradient on relief-based exposure to solar radiation also in Turku. In addition, there are no significant topographically induced local winds that would amplify the relief influence (cf. Goldreich, 1984).

On a monthly and annual basis, the impact of topography manifests itself in the negative correlation between relative elevation and diurnal temperature range. Compared to the corresponding effect of water bodies and urban land use, the effect is, however, weaker. In the Turku area, daily minimum temperatures are lowest in relatively low positions, whereas daily maximum temperatures are lowest in relatively high positions (**I**: Table 4). This reflects the typical diurnal variation in atmospheric stratification, i.e. nocturnal inversions as opposed to normal atmosphere during daytime. Modelling results indicate that relief-induced inversion is a more important climatic factor than the thermal effect of topography during normal atmospheric stratification (**I**: Table 5; **III**: Table 2). As a consequence of these contrasting impacts during inversions and normal atmospheric stratification, the effect of relative elevation on *average* temperatures is rather neutral. In March (**I**: Table 5a; **IV**: Table 7) and April (**I**: Table 5a), however, the relative elevation variable was included in the linear regression model of average temperatures, indicating higher temperatures at higher positions. As discussed in the context of model performances in general, the largest relative importance of topography in early spring is explained at least partly by conditions favourable to inversions, when the snow cover still remains, while the air temperature gets higher towards the summer (cf. Nkemdirim, 1976; Paterson and Hage, 1979).

The effect of topography in the Turku area is not uniform in urban and rural areas. In line with the observations of e.g. Kuttler et al. (1996), low-lying rural places seem to be more prone to cold air drainage than corresponding urban places. This pattern was identified in monthly and annual data as well as in momentary situations. The marketplace (Figure 9), which had the highest daily minimum temperatures in each month, is located in a relatively low-lying valley. The rural inland place Niuskala (Figure 9), which had the lowest daily minima in each month, occupies a topographically rather similar environment. During the study periods, the inversion occasionally prevailed in the city centre, but more often in rural areas. In some cities, the influence of topography can outperform that of the urban effect (Chandler, 1964), but around the Turku grid plan area, in the long term, the impact of land use dominates.

Although the impact of topography does not dominate as a long-term climatic component in the Turku area, its effect is pronounced during stable atmospheric conditions. For example, during cold winter weather, the maximum temperature difference of 10 ºC was observed within 3 km distance between the warm city centre and the coldest place, a topographic low in Halinen (Figure 7 and Table 3, site no. 44; Figure 9; **IV**: Figure 11a). Another example comes from the marketplace, which in the long term is the warmest site in the study region: now it was colder than the partly park-covered surrounding hills, indicating a stronger impact of topography than of the urban complex. A similar spatial temperature distribution that deviates from the long-term average temperature pattern

occasionally also existed during other inversion situations of the study periods, being more common and intensive in winter (cf. Lazar and Podesser, 1999).

In general, the results concerning the effect of topography on spatial temperature differences also depend on the topographic variable. As the effect of relative elevation is pronounced during stable atmospheric conditions, the influence of altitude increases with cloudy and windy weather, when the impacts of other factors on temperature differences are rather small (Bogren et al., 2000). For example, in Gothenburg, Sweden, Eliasson and Svensson (2003) report that the effect of altitude is more important than that of land use during cloudy and windy conditions. In Turku, too, a relatively large impact of altitude was observed during cloudy and windy winter weather with normal atmospheric stratification: the highest places were also the coldest even if the surrounding land use was not particularly rural. Generally, as the relief in the Turku area is relatively gentle, also the altitude-based temperature differences during a normal stratospheric stratification are rather small.

5.3.3. Land use

The effect of land use on temperature is a challenging task. Land use varies in the real world sometimes abruptly, sometimes gradually, making classification difficult. The land use classification scheme itself is somewhat ambiguous, and there are different standards e.g. in different countries. In this study, employing the SLICES data set, land use was approached from two main view angles: 1) to distinguish the true 'urban effect' from other factors affecting the local climate in the Turku area; and 2) to assess the independent effect and modelling performance of various land use classes and their combinations. Consequently, the type of the land use variables used represented a continuum from urban to rural variables, with a 'grey zone' of types which could be attributed to either end of the spectrum. The variables reflecting urban impact are called "urban land use" in this section.

In general, urban land use was found to increase temperatures throughout the year. Diurnally, urban land use raised the daily minimum and maximum temperatures and thereby also daily average temperatures. It also decreased the diurnal temperature range. The urban cold island detected in spring and summer, however, refers to the thermal inertia of urban areas during seasons of large diurnal temperature variation and the strong role of solar radiation as a climatic agent. Therefore, the impact of urban land use is not necessarily a warming one throughout the day. The thermal inertia is not strong enough to affect the daily maximum temperature models of spring and summer months (**I**: Table 5c; **III**: Table 2). This is interpreted to result from the sea–land breeze circulation, which is another factor producing the daytime urban cold island. In addition, the daily maximum temperatures are generally reached in the afternoon (**IV**: Figure 5),

whereas the impacts of thermal inertia are most clearly seen already before noon (**IV**: Figure 12).

The impact of urban land use on temperatures was generally stronger than that of water bodies and topography. During the seasons of relatively cold and warm sea, however, the effect of water bodies was of the same magnitude, and especially in daytime in spring, the water body impact outperformed that of the urban land use (**I**: Table 5; **III**: Table 2; **IV**: Table 7). In relation to topography, the long-term impact of land use was stronger throughout the year and the day. Only in momentary situations, such as wintertime inversions, did the impact of topography locally exceed that of urban land use (**IV**).

The urban variables employed in the study were selected from the SLICES data set, either as original land use classes or specifically produced class combinations. Building floor areas were used as a supplementary data set in the analyses. Selection was based on the estimated thermal effect of the land use classes, or correlation between temperatures and land use classes. In paper **IV**, the strongest variable from the group of potential intercorrelated variables was filtered with the HP method. In general, combinations of original land use classes performed better than the single classes, reflecting the level of detail of the original classification. Land use variables typically outperformed the floor area variable (**III**: Table 2; **IV**: Figure 4, Table 5). In the ranking of independent effects of the urban variables with the HP method, the building-based variables outperformed the variables consisting of traffic areas, or combinations of buildings and traffic areas. This demonstrates that heat flux from buildings is a more important factor than heat release from horizontal urban surfaces. The difference between the relative importance of horizontal urban surfaces and buildings was smallest during the months of the large solar heating, albeit also then, the buildings were more important (**IV**: Figure 4). It is worth noting that the variables do not necessarily behave similarly in the model and in the HP analysis. In addition, the spatial scale seems to influence the relative strengths of the variables. For example, a 100 x 100 m floor area grid cell may be too small for the floor area variable to perform optimally as a part of a model (**III**: Table 2; cf. Eliasson and Svensson, 2003).

In papers **I** and **III**, the land use variables reflected the urban effect, while in paper **IV**, non-urban and intermediate variables were also analysed. An example of the intermediate variables is industrial land use, denoting places that are traditionally considered a noteworthy source of anthropogenic heat (e.g. Hart and Sailor, 2009) and hence, speak for its definition as an urban variable. The correlations between industrial areas and temperatures were positive, but weaker than other variables classified as urban. Based on the HP results, industrial areas seem to have only a minor independent effect on temperatures in the Turku area. The relatively low thermal significance of industrial areas reflects the fact that the industry in the area is mainly light, and the impact comes mainly

across the extra heat from industrial buildings and artificial surfaces in the industrial areas, whereas the role of industrial burning processes is minor. An example of a clearly non-urban variable is the satellite image-based 'greenness' index. In our preliminary analysis, 'greenness' outperformed the NDVI (Normalized Difference Vegetation Index), which has been used in earlier UHI studies e.g. by Chen et al. (2006) and Szymanowski and Kryza (2011) and was hence included in the further analyses. In HP, 'greenness' had the second strongest independent effect on temperatures, second only to the urban variable (**IV**: Table 6). As part of the linear regression model, the greenness variable also had strong relative explanatory power, especially in summer (**IV**: Table 7). Contrary to the effect of the urban variable, the effect of 'greenness' on temperatures was naturally negative, indicating increased evapotranspiration and lack of anthropogenic heat sources and artificial surfaces. Based on our experience, 'greenness' is indeed a potential variable in the UHI modelling context. Since it is a spatially continuous variable, the probability to multicollinearity problems can be considered smaller than among the variables based on the proportional area of certain land cover (cf. Kolokotroni and Giridharan, 2008).

6. SOCIETAL RELEVANCE OF UHI RESEARCH IN TURKU AND POTENTIAL FUTURE RESEARCH TOPICS

The results of this study can be utilised in city planning on different spatial and temporal scales, for example, in the estimation of spatial differences in heating demand and the need for slip-prevention measures. In urban areas with their longer growing season, it is possible to take this into account when estimating the niches of suitable plants e.g. for urban parks. The TURCLIM project collaborates with the Turku Environment and City Planning Department, supporting the utilisation of climate information in municipal decision making. The city of Turku collects data on air quality in the city and its neighbouring municipalities, and the collaboration enables research on the combined effects of UHI and air quality in the area.

Climate change may alter the characteristics of UHI. So far, the predictions concerning the connections between UHI intensity and climate change have not been unanimous. On the one hand, it has been predicted that the night-time temperatures will rise less in urban than in rural areas, resulting in weaker UHI (Oleson et al., 2011). On the other hand, opposite results predicting an intensifying of UHI have been reported (see Wilby, 2003). Regardless of the future trend in UHI intensity, the temperatures in urban areas will rise as a consequence of a general warming trend. In winter, the effect can be considered mostly positive, while in summer, heat stress will become a more concrete problem also at high latitudes.

From the beginning of September 2012 to the end of October 2014, the Department of Geography and Geology at the University of Turku participated, together with the city of Turku, in the ERDF-funded national project "Climate-Proof City (ILKKA) – Tools for Planning", which had altogether seven actors also including FMI, the Helsinki Region Environmental Services Authority and the cities of Helsinki, Vantaa and Lahti. The leading theme of the project was to develop climate change adaptation and mitigation tools for city planners. The University of Turku collaborated with the city of Turku and FMI in a work package analysing UHI and its characteristics in a changing climate. The UHI was analysed together with air quality and weather, and one aim was to identify the weather conditions which bring about poor air quality and, together with high UHI intensity, cause a high risk of heat stress-induced health problems. Combining land use information and temperature maps allowed the detection of areas sensitive to climate-driven health risks. As an adaptive measure it is not appropriate to locate hospitals or elderly care services to these risk areas. From the viewpoint of mitigation, information on spatial temperature differences can be utilised in planning a more energy-efficient city

e.g. by building in regions where the need for wintertime heating and summertime cooling could be minimised. Improved understanding of the spatio-temporal characteristics of UHI achieved in this study will be utilised in further analyses in the Turku area.

In many cities, knowledge about intra-urban and urban-rural temperature differences is still rather incomplete. The GIS-based modelling methods applied in this study offer a cost-effective way to estimate spatial temperature differences in areas where *in situ* observations are not available. One benefit of the GIS-based modelling is that data sets are often available from large areas, enabling cost-effective testing and the potential for extrapolation of the models into environments that have sparse temperature measurement networks.

Another identified future research topic is the impact of sea ice cover on the spatio-temporal behaviour of UHI. The extent of sea ice cover can have large annual variation. Ice thickness can also vary remarkably depending, for example, on the snow accumulation rate after the formation of a permanent ice cover. Differences in ice cover affect the spatio-temporal temperature pattern in the area, demonstrated, for example, in the spatial shift of the relatively warm or cold regions. To better understand the role of thermal inertia and land–sea breeze circulation in the formation of daytime UCI necessitates more research in the Turku area. With respect to weather, and thermal inertia, case studies of rapid temperature changes would bring more information on the UHI dynamics. Vertical temperature measurements would bring more detailed information on UHI thickness and the role of topography in UHI formation in different weather conditions. The increased use of remote sensing in UHI studies has engendered novel research settings. Connections between land surface temperature, land use and air temperature call for further investigations. One potential application would be to test the applicability of land surface temperature, either simultaneously or with a proper time gap, as a predictor in an air temperature model in the Turku area (cf. Schwarz et al., 2012).

7. CONCLUSIONS ABOUT UHI DYNAMICS IN THE STUDY AREA

Timing

The UHI in the Turku area is generally strongest at night and at the end of summer. The strongest momentary UHI intensities are, however, met in winter, when UHI commonly prevails throughout the day. In summer, a daytime urban cold island is common. Diurnal UHI intensity variation is larger and more regular in summer than in winter, reflecting differences in seasonal importance of solar heat storage and anthropogenic heat release as the principal drivers of UHI.

Location

The marketplace and its densely built surroundings in the city centre are the warmest region in the Turku area. The coldest sites are rural inland places slightly over 10 km to the north-east of the city centre. This general spatial pattern is, however, broken in certain conditions, for example in daytime in spring and in summer, when the warmest sites are found in semi-urban and rural places, causing a UCI. On average, the UHI intensity in the Turku area is 1.9 °C, while occasionally the temperature excess of the city centre in relation to the surroundings can be up to 10 °C. The UCI intensity in the area is significantly weaker, typically less than 2 °C.

Causes

Land use is the most significant factor bringing about spatial temperature differences in the study area. The impact of water bodies is pronounced in spring and autumn. While the effect of urban land use is typically warming throughout the year, water bodies have a twofold impact; in spring, the relatively cold sea lowers the daytime temperatures in the coastal zones. The cooling impact extends also to the city centre, being one factor promoting the daytime urban cold island observed in spring and summer. In autumn the sea temperature is relatively high, and the coastal areas are the warmest, second only to the city centre. In the long term, topography had least impact on temperatures. In the short term, during stable atmospheric stratification, the impact of topography can occasionally outperform that of land use. Relief impact materialises mainly as night-time cold air drainage to relatively low-lying places.

Influence of weather

UHI intensity in Turku is negatively correlated with wind speed and cloudiness. Wind speed seems to be the more critical factor in suppressing the intensity of UHI. When the

wind speed exceeded 3 m/s, UHI intensities remained below 2 °C, while a UHI of 6 °C may exist even with total cloudiness of 6/8.

Model performance

Modelling results suggest that it is possible to predict spatial temperature differences in the Turku region based on various environmental variables. Among linear regression models, the explanatory power of average temperature, daily minimum temperature and diurnal temperature range models was in general higher than the explanatory power of the daily maximum model. In a methodological comparison of BRT and GLM, the diurnal superiority of the models was not as clear, even though the model calibration succeeded less often in daily maximum temperatures and also the model evaluation results were in general poorest with the daily maxima. Generally, in the comparison between BRT and GLM, the GLM performed better and indicated that for small sample sizes, parametric statistical techniques should be preferred over non-parametric methods.

Modelling scale

New results about the scale of environmental variables support the earlier estimations of the proper source area in urban environments. The statistically determined optimal buffer sizes of urban variables were either 300 m or 1000 m, thus fitting within the scale that has been applied in earlier UHI studies (e.g. Giridharan et al., 2008, Wen et al., 2011). The determined buffer sizes are in line with Oke's (2006) estimation of 0.5 km as an approximate circle of influence area for screen level temperature measurements.

Among non-urban variables, the optimal buffer sizes had a larger spatial scale extending from 100 m to 20000 m. Compared to urban variables, the mode and average of the determined buffer sizes were larger. The observation fits Giridharan and Kolokotroni's (2009) and Stewart and Oke's (2009) considerations of the appropriateness of a larger buffer size in a natural or sparsely built environment compared to densely built urban areas.

Seasonally, the optimal buffer sizes of the urban variables behaved rather uniformly. The circle of influence was largest in spring and smallest in autumn and winter. This pattern is in line with the opinion of Giridharan and Kolokotroni (2009), who conclude that in summer studies, the source area for urban variables should be larger than in winter. Among non-urban variables, the seasonal pattern varied, and a uniform trend was not observed.

8. REFERENCES

Ackerman B. (1985) Temporal march of the Chicago heat island. Journal of Climate and Applied Meteorology 24: 547–554.

Aida M. (1982) Urban albedo as a function of the urban structure – a model experiment. Boundary-Layer Meteorology 23: 405–414.

Akbari H. and Konopacki S. (2004) Energy effects of heat-island reduction strategies in Toronto, Canada. Energy 29: 191–210.

Akbari H., Matthews H.D. and Seto D. (2012) The long-term effect of increasing the albedo of urban areas. Environmental Research Letter 7 024004: 10 pp.

Alcoforado M.J. and Andrade H. (2006) Nocturnal urban heat island in Lisbon (Portugal): main features and modelling attempts. Theoretical and Applied Climatology 84:151-159.

Arnfield A.J. (2003) Two decades of urban climate research: a review of turbulence, exchanges of energy and water, and the urban heat island. International Journal of Climatology 23: 1-26.

Arvola E. (1987) Air flow patterns and weather types affecting the climate of Finland. In Alalammi, P. (ed.), Atlas of Finland 131. Climate. National Board of Survey, Geographical Society of Finland, Helsinki.

Atkinson B.W. (2003) Numerical modelling of urban heat-island intensity. Boundary-Layer Meteorology 109: 285–310.

Barry R.G. and Chorley R.J. (1998) Atmosphere, Weather and Climate. 7th edition. 409 pp. Routledge, London.

Bogren J., Gustavsson T. and Postgård U. (2000) Local temperature differences in relation to weather parameters. International Journal of Climatology 20: 151–170.

Bokwa A. (2011) Impact of relief on air temperature in urban area. Prace i Studia Geograficzne T. 47: 347–354.

Bornstein R.D. (1968) Observations of the urban heat island effect in New York City. Journal of Applied Meteorology 7: 575–582.

Bottyán Z. and Unger J. (2003) A multiple linear statistical model for estimating the mean maximum urban heat island. Theoretical and Applied Climatology 75: 233–243.

Bowling S.A. and Benson C.S. (1978) Study of the Subarctic Heat Island at Fairbanks, Alaska. Environmental Protection Agency Report, EPA600/4-78-027.

Brown D.J., Shepherd K.D., Walsh M.G., Mays M.D. and Reinsch T.G. (2006) Global soil characterization with VNIR diffuse reflectance spectroscopy. Geoderma 132: 273–290.

Brown L.C. and Duguay C. R. (2010) The response and role of ice cover in lake–climate interactions. Progress in Physical Geography 34: 5, 671–704.

Buechley R.W., Van Bruggen J. and Truppi L.E. (1972) Heat islands = Death island? Environmental Research 5:85–92.

Chandler T.J. (1964) City growth and urban climate. Weather 19: 170–171.

Chapman L. and Thornes J.E. (2003) The use of geographical information systems in climatology and meteorology. Progress in Physical Geography 27: 313–330.

Charabi Y., Bakhit A. (2011) Assessment of the canopy urban heat island of a coastal arid tropical city: The case of Muscat, Oman. Atmospheric Research 101 (1–2): 215–227.

Chen L., Ng E., An X., Ren C., Lee M., Wang U. and Zhengjun H. (2012) Sky view factor analysis of street canyons and its implications for daytime intra-urban air temperature differentials in high-rise, high-density urban areas of Hong Kong: a GIS-based simulation approach. International Journal of Climatology 32: 121–136.

Chen X.-L., Zhao H.-M., Li P.-X. and Yin Z.-Y. (2006) Remote sensing image-based analysis of the relationship between urban heat island and land use/cover changes. Remote Sensing of Environment 104:133–146.

Christen A. and Vogt R. (2004) Energy and radiation balance of a central European city. International Journal of Climatology 24: 1395–1421.

Cleugh H.A. and Oke T.R. (1986) Suburban-rural energy balance comparisons in summer for Vancouver, B.C. Boundary-Layer Meteorology 36: 351–369.

Conti S., Meli P., Minelli G., Solmini R., Toccaceli V., Vichi M., Beltrano C. and Perini L. (2005) Epidemiologic study of mortality during the summer

2003 heatwave in Italy. Environmental Research 98(3): 390–399.

Costa A., Labaki L., Araujo V. (2007) A methodology to study the urban distribution of air temperature in fixed points. In: Santamouris M., Wouters P. (eds) 2nd PALENC and 28th AIVC Conference: Building Low Energy Cooling and Advanced Ventilation Technologies in the 21st Century, 27–29 Sep 2007, Crete, p 227–230.

Cotton W.R. and Pielke R.A. (1995) Human Impacts on Weather and Climate. Cambridge University Press: Cambridge.

EEA (European Environment Agency) (2006) CORINE land cover. EEA, Denmark

EIA (2005) Annual Energy Review 2005DOE/EIA-0384.

Ekholm J. (1981) Joensuun paikallisilmasto. Terra 93(4): 145–154.

Eliasson I. (1996) Intra-urban nocturnal temperature differences: a multivariate approach. Climate Research 7: 21–30.

Eliasson I. and Svensson M.K. (2003) Spatial air temperature variations and urban land use – a statistical approach. Meteorological Applications 10: 135–149.

Elith J., Leathwick J.R. and Hastie T. (2008) A working guide to boosted regression trees. Journal of Animal Ecology 77:802–813.

Emmanuel R. and Krüger E. (2012) Urban heat island and its impact on climate change resilience in a shrinking city: The case of Glasgow, UK. Building and Environment 53: 137–149.

Erell E., Pearlmutter D. and Williamson T. (2011) Urban Microclimate. Designing the Spaces Between Buildings. 288 pp. Earthscan, UK.

Fan H. and Sailor D.J. (2005) Modeling the impacts of anthropogenic heating on the urban climate of Philadelphia: a comparison of implementations in two PBL schemes. Atmospheric Environment 39 (1): 73-84.

FAO (1983) Solar energy in small-scale milk collection and processing. FAO Animal Production and Health Paper 39. Food and Agriculture Organization of the United Nations Rome, 1983. <http://www.fao.org/docrep/003/x6541e/X6541E03.htm> 9.11.2013.

Fogelberg P., Nikiforow M., Söderman G. and Tornberg L. (1973) Havaintoja Helsingin talvisesta lämpöilmastosta. Terra 85(4): 234–239.

Freitas D.E., Rozoff C.M., Cotton W.R. and Dias P.L.S. (2007) Interactions of an urban heat island and sea-breeze circulations during winter over the metropolitan area of São Paulo, Brazil. Boundary-Layer Meteorology 122: 43–65.

Gago E.J., Roldan J., Pacheco-Torres R. and Ordóñez J. (2013) The city and urban heat islands: a review of strategies to mitigate adverse effects. Renewable and Sustainable Energy Reviews 25: 749–758.

Gál T. and Unger J. (2009) Detection of ventilation paths using high-resolution roughness parameter mapping in a large urban area. Building and Environment 44: 198–206.

Ganbat G., Han J.-Y., Ryu Y.-H. and Baik J.-J. (2013) Characteristics of the urban heat island in a high-altitude metropolitan city, Ulaanbaatar, Mongolia. Asia-Pacific Journal of Atmospheric Sciences 49(4): 535–541.

Geiger R., Aron R.H. and Todhunter P. (1995) The Climate Near the Ground, 5th edition. 528 s. Braunschweig/Wiesbaden.

Georgescu M., Morefield PE, Bierwagen BG, Weaver CP. 2014. Urban adaptation can roll back warming of emerging megapolitan regions. Proceedings of the National Academy of Sciences of the United States of America. PNAS Early Edition. <www.pnas.org/cgi/doi/10.1073/pnas.1322280111>. 20.3.2014.

Giridharan R., Lau S.S.Y, Ganesan S. and Givoni B. (2007) Urban design factors influencing heat island intensity in high-rise high-density environments of Hong Kong. Building and Environment 42: 3669–3684.

Giridharan R., Lau S.S.Y, Ganesan S. and Givoni B. (2008) Lowering the outdoor temperature in high-rise high-density residential developments of coastal Hong Kong: vegetation influence. Building and Environment 43: 1583−1595.

Giridharan R. and Kolokotroni M. (2009) Urban heat island characteristics in London during winter. Solar Energy 83: 1668–1682.

Gobakis K., Kolokotsa D., Synnefa A., Saliari M., Giannopoulou K. and Santamouris M. (2011) Development of a model for urban heat island prediction using neural network techniques. Sustainable Cities and Society 1: 104–115.

Goldreich Y. (1969) A preliminary study of aspects of Johannesburg's urban climate. University of the Witwatersrand, unpublished PhD thesis.

Goldreich Y. (1971) Influence of topography on Johannesburg's temperature distribution. South African Geographical Journal 53: 84-88.

Goldreich Y. (1984) Urban topoclimatology. Progress in Physical Geography 8: 336–364.

Grimmond C.S.B., Oke T.R. (1999) Heat storage in urban areas: local-scale observations and evaluation of a simple model. Journal of Applied Meteorology 38: 922–940.

Hamilton I.G., Davies M., Steadman P., Stone A., Ridley I. and Evans S. (2009) The significance of the anthropogenic heat emissions of London's buildings: a comparison against captured shortwave solar radiation. Building and Environment 44: 807–817.

Hart M.A. and Sailor D.J. (2009) Quantifying the influence of land-use and surface characteristics on spatial variability in the urban heat island. Theoretical and Applied Climatology 95: 397–406.

Hathway E.A. and Sharples S. (2012) The interaction of rivers and urban form in mitigating the urban heat island effect: a UK case study. Building and Environment 58: 14–22.

He G.-X., Yu C.W.F., Lu C. and Deng Q.H. (2013) The influence of synoptic pattern and atmospheric boundary layer on PM10 and urban heat island. Indoor and Built Environment 22(5): 796–807.

Heino R. (1978) Urban effect on climatic elements in Finland. Geophysica 15(2): 171–188.

Hinkel K.M., Nelson F.E., Klene A.E. and Bell J.H. (2003) The urban heat island in winter at Barrow, Alaska. International Journal of Climatology 23: 1889–1905.

Hjort J. and Marmion M. (2008) Effects of sample size on the accuracy of geomorphological models. Geomorphology 102: 341–350.

Hjort J. and Luoto M. (2009) Interaction of geomorphic and ecologic features across altitudinal zones in a subarctic landscape. Geomorphology 112: 324–333.

Hjort J. and Marmion M. (2009) Periglacial distribution modelling with a boosting method. Permafrost and Periglacial Processes 20: 15–25.

Hjort J., Etzelmüller B. and Tolgensbakk J. (2010) Effects of scale and data source in periglacial distribution modelling in a High Arctic environment, western Svalbard. Permafrost and Periglacial Processes 21: 345–354.

Huovila S. (1987) Microclimate. In Alalammi, P. (ed.), Atlas of Finland 131. Climate. National Board of Survey, Geographical Society of Finland, Helsinki.

Ichinose T., Shimodozond K. and Hanaki K. (1999) Impact of anthropogenic heat on urban climate in Tokyo. Atmospheric Environment 33, 3897–3909.

Itämeriportaali (2014) Itämeriportaali. Finnish Environment Institute SYKE, The Finnish Meteorological Institute, Ministry of the Environment. <http://www.itameriportaali.fi> 23.2.2014.

Jaakkola O. and Helminen V. (2002) Usability of the SLICES land-use database. 5th AGILE Conference on Geographic Information Science, Palma (Balearic Islands, Spain) April 25th–27th 2002. <http://itcnt05.itc.nl/agile_old/Conference/mallorca2002/proceedings/dia25/Session_4/s4_Jaakkola.pdf> 8.3.2014.

Jochner S.C., Sparks T.H., Estrella N. and Menzel A. (2012) The influence of altitude and urbanisation on trends and mean dates in phenology (1980–2009). International Journal of Biometeorology 56(2): 387–94.

Johansson M.M., Pellikka H., Kahma K.K., Ruosteenoja K. (2014) Global sea level rise scenarios adapted to the Finnish coast. Journal of Marine Systems 129: 35–46.

Jongtanom Y., Kositanont C. and Baulert S. (2011) Temporal variations of urban heat island intensity in three major cities.Thailand. Modern Applied Science 5: 105–110.

Khan S.M. and Simpson RW. (2001) Effect of a heat island on the meteorology of a complex urban airshed. Boundary-Layer Meteorology 100:487–506.

Kim Y.-H. and Baik J.-J. (2002) Maximum urban heat island intensity in Seoul. Journal of Applied Meteorology 41:651–659.

Kim Y.-H. and Baik J.-J. (2005) Spatial and temporal structure of the urban heat island in Seoul. Journal of Applied Meteorology 44(5): 591–605.

Klysik K. (1996) Spatial and seasonal distribution of anthropogenic heat emissions in Lodz, Poland. Atmospheric Environment 30: 3397–3404.

Klysik K. and Fortuniak K. (1999) Temporal and spatial characteristics of the urban heat island of Lodz, Poland. Atmospheric environment 33: 3885–3895.

Kolokotroni M. and Giridharan R. (2008) Urban heat island intensity in London: an investigation of the impact of physical characteristics on changes in outdoor air temperature during summer. Solar Energy 82: 986–998.

Kolokotroni M., Davies M., Croxford B., Bhuiyan, S. and Mavrogianni A. (2010) A validated methodology for the prediction of heating and cooling energy demand for buildings within the urban heat island: case study of London. Solar Energy 84: 2246–2255.

Kuttler W., Barlag A.-B. and Rossmann F. (1996) Study of the thermal structure of a town in a narrow valley. Atmospheric Environment 30(3): 365–378.

Laaksonen K. (1994) Lämpötilan jakaumia Hyvinkään kaupungissa keskikesän öinä. Terra 106(3): 326–342.

Lai L.-W., Cheng W.-L. (2009) Air Quality influenced by urban heat island coupled with synoptic weather patterns. Science of the Total Environment 407: 2724-2733.

Landsberg H.E. (1981) The Urban Climate. Academic Press: London.

Lazar R., Podesser A. (1999) An urban climate analysis of Graz and its significance for urban planning in the tributary valleys east of Graz (Austria). Atmospheric Environment 33: 4195–4209.

Lee S.-J., Balling R. and Gober P. (2008) Bayesian maximum entropy mapping and the soft data problem in urban climate research. Annals of the Association of American Geographers 98(2): 309–322.

Lee J.S., Kim J.T. and Lee M.G. (2013) Mitigation of urban heat island effect and greenroofs. Indoor and Built Environment 000;000:1–8.

Li S., Mo H. and Dai Y. (2011) Spatio-temporal pattern of urban cool island intensity and its eco-environmental response in Chang-Zhu-Tan urban agglomeration. Communications in Information Science and Management Engineering 1: 1–6.

Lindberg F., Grimmond C.S.B., Yogeswaran N., Kotthaus S. and Allen L. (2013) Impact of city changes and weather on anthropogenic heat flux in Europe 1995–2015. Urban Climate 4: 1–15.

Lindqvist S. (1970) Bebyggelseklimatologiska Studier. Meddelande fådn Lunds Universitets Geografiska Institution, Avhandlingar LXI, Gleerup, Lund (with summary in English).

Lu P., Yu Q., Liu J. and Lee X. (2006) Advance of three-flowering dates in response to urban climate change. Agricultural and Forest Meteorology 138: 120–131.

Luoto M. and Hjort J. (2006) Scale matters – a multi-resolution study of the determinants of patterned ground activity in subarctic Finland. Geomorphology 80 (3–4): 282–294.

Magee N., Curtis J. and Wendler G. (1999) The urban heat island effect at Fairbanks, Alaska. Theoretical and applied climatology 64: 39–47.

Matzarakis A., Muthers S. and Koch E. (2011) Human biometeorological evaluation of heat-related mortality in Vienna. Theoretical and Applied Climatology 105(1-2): 1–10.

Memon R.A. and Leung D.Y.C. (2010) Impacts of environmental factors on urban heating. Journal of Environmental Sciences 22(12): 1903–1909.

Miara K., Paszyfiski J. and Grzybowski J. (1987) Zrózniicowanie przestrzenne bilansu promieniowania na obszarze Polski. Przegled Geogr. t. LIX, z. 4

Mirzaei P.A. and Haghighat F. (2010) Approaches to study urban heat island – abilities and limitations. Building and Environment 45: 2192–2201.

Morris C.J.G. and Simmonds I. (2000) Associations between varying magnitudes of the urban heat island and the synoptic climatology in Melbourne. Australia. International Journal of Climatology 20: 1931–1954.

Morris C.J.G., Simmonds I. and Plummer N. (2001) Quantification of the influences of wind and cloud on the nocturnal urban heat island of a large city. Journal of Applied Meteorology 40: 169–182.

Myrup L.O., McGinn C.E. and Flocchini R.G. (1993) An analysis of microclimate variation in a suburban environment. Atmospheric Environment, Part B. Urban atmosphere 27 (2): 129–156.

NASA (2004) NASA/Goddard Space Flight Center. 'Urban Heat Islands Make Cities Greener.' ScienceDaily, 30 Jul. 2004. <http://www.sciencedaily.com /releases/2004/07/040730085916.htm> 1.11.2013.

Nkemdirim L.C. (1976) Dynamics of an urban temperature field – a case study. Journal of Applied Meteorology 15: 818–828.

Nkemdirim L.C. (1980) A test of a lapse rate/wind speed model for estimating heat island magnitude in an urban airshed. Journal of Applied Meteorology 19: 748–756.

Nkemdirim L.C., Truch P. and Leggat K. (1977) Calgary urban heat island 1975 – surface features. Weather Research Monograph 1, University of Calgary. 80 pp.

NLS (National Land Survey of Finland) (2009) Digital elevation model. NLS, Helsinki

Näyhä S. (2007) Heat mortality in Finland in the 2000s. International Journal of Circumpolar Health 66(5): 418–424.

Oke T.R. (1973) City size and the urban heat island. Atmospheric Environment 7: 769–779. DOI:10.1016/0004-6981(73)90140-6

Oke T.R. (1976) The distinction between canopy and boundary-layer urban heat islands. Atmosphere 14(4): 268-277.

Oke T.R. (1981) Canyon geometry and the urban heat island: comparison of scale model and field observations. International Journal of Climatology 1: 237–254.

Oke T.R. (1987) Boundary Layer Climates, 2nd edition. 435 pp. Routledge, London.

Oke T.R. (1988) The urban energy balance. Progress in Physical Geography 12: 471–508.

Oke T.R. (2006) Initial Guidance to Obtain Representative Meteorological Observations at Urban Sites. Instruments and Observing Methods Report No. 81. World Meteorological Organization, Geneva.

Oke T.R. and Maxwell G.B. (1975) Urban heat island dynamics in Montreal and Vancouver. Atmospheric Environment 9: 191–200.

Oleson K., Bonan G.B., Feddema J. and Jackson T. (2011) An examination of urban heat island characteristics in a global climate model. International Journal of Climatology 36: 1848–1865.

Onset (2013) Onset Hobo data loggers. <http://www.onsetcomp.com/> 31.10.2013.

Papanastasiou D.K. and Kittas C. (2012) Maximum urban heat island intensity in a medium-sized coastal Mediterranean city. Theoretical and Applied Climatology 107: 407–416.

Parris K.M. and Hazell D.L. (2005) Biotic effects of climate change in urban environments: the case of the grey-headed flying-fox (Pteropus poliocephalus) in Melbourne, Australia. Biological Conservation 124(2): 267–276.

Paterson R.D. and Hage K.D. (1979) Micrometeorological study of an urban valley. Boundary-Layer Meteorology 17: 175–186.

Peel M.C., Finlayson B.M. and McMahon T.A. (2007) Updated world map of the Köppen-Geiger climate classification. Hydrology and Earth System Sciences 11: 1633–1644.

Pike G., Pepin N.C. and Schaefer M. (2013) High latitude local scale temperature complexity: the example of Kevo Valley, Finnish Lapland. International Journal of Climatology 33(8): 2050–2067.

Pirinen P., Simola H., Aalto J., Kaukoranta J.-P., Karlsson P. and Ruuhela R. (2012) Tilastoja Suomen ilmastosta 1981–2010. Ilmatieteen laitos, raportteja 2012: 1.

Preston-Whyte R.A. (1973) Wind modification of temperature and moisture distributions over Durban. South African Geographer 4, 203–209.

Priyadarsini R., Wong N.H. and Cheong K.W. (2008) Microclimatic modelling of the urban thermal environment of Singapore to mitigate urban heat island. Solar Energy 82(8): 727–745.

Quah A.K.L. and Roth M. (2012) Diurnal and weekly variation of anthropogenic heat emissions in a tropical city, Singapore. Atmospheric Environment 46: 92–103.

Saaroni H., Ben-Dor E., Bitan A. and Potchter O. (2000) Spatial distribution and microscale characteristics of the urban heat island in TelAviv, Israel. Landscape and Urban Planning 48: 1–18.

Saaroni H. and Ziv B. (2003) The impact of a small lake on heat stress in a Mediterranean urban park: the case of Tel Aviv, Israel. International Journal of Biometeorology 47: 156–165.

Sailor D.J. (2011) A review of methods for estimating anthropogenic heat and moisture emissions in the urban environment. International Journal of Climatology 31 (2): 189–199.

Sailor D.J. and Lu L. (2004) A top-down methodology for developing diurnal and seasonal anthropogenic heating profiles for urban areas. Atmospheric Environment 38: 2737–2748.

Sailor D.J. and Hart M. (2006) An anthropogenic heating database for major U.S. cities. 6th Symposium on the Urban Environment, Atlanta. American Meteorological Society.

Sakakibara Y. and Matsui E. (2005) Relation between heat island intensity and city size indices/urban canopy characteristics in settlements of Nagano basin, Japan. Geographical Review of Japan 78: 812−824.

Salamanca F., Krpo A., Martilli A. and Clappier A. (2010) A new building energy model coupled with an urban canopy parameterization for urban climate simulations – Part I. formulation, verification and sensitivity analysis of the model. Theoretical and Applied Climatology 99: 331–344.

Schwarz N., Schlink U., Franck U. and Grossmann K. (2012) Relationship of land surface and air temperatures and its implications for quantifying urban heat island indicators – an application for the city of Leipzig (Germany). Ecological Indicators 18: 693–704.

Siu W.L. and Hart M.A. (2013) Quantifying urban heat island intensity in Hong Kong SAR, China. Environmental Monitoring and Assessment 185: 4383–4398.

SLICES (2006) SLICES land use database. National Land Survey of Finland.

Solecki W.D., Rosenzweig C., Pope G., Chopping M., Goldberg R. and Polissar A. (2004) Urban heat island and climate change: an assessment of interacting and possible adaptations in the Camden, New Jersey Region. Environmental Assessment and Risk Analysis Element. Research Project Summary. 5 pp.

Somers K.A., Bernhardt E.S., Grace J.B., Hassett B.A., Sudduth E.B., Wang S. and Urban D.L. (2013) Streams in the urban heat island: spatial and temporal variability in temperature. Freshwater Science 32(1): 309–326.

Souch C. and Grimmond S. (2006) Applied climatology: urban climate. Progress in Physical Geography 30(2): 270–279.

Spronken-Smith R.A. and Oke T.R. (1999) Scale modelling of nocturnal cooling in urban parks. Boundary-Layer Meteorology 93: 287–312.

Steeneveld G.J., Koopmans S., Heusinkveld B.G., van Hove L.W.A. and Holtslag A.A.M. (2011) Quantifying urban heat island effects and human comfort for cities of variable size and urban morphology in the Netherlands. Journal of Geophysical Research 116, D20129.

Steeneveld G.J., Koopmans S., Heusinkveld B.G. and Theeuwes N.E. (2014) Refreshing the role of open water surfaces on mitigating the maximum urban heat island effect. Landscape and Urban Planning 121: 92–96.

Steinecke K. (1999) Urban climatological studies in Reykjavik, subarctic environment, Iceland. Atmospheric Environment 33: 4157–4162.

Stewart I.D. and Oke T.R. (2009) Classifying urban climate field sites by 'local climate zones': the case of Nagano, Japan. In: Preprints, 7th Int Conf Urban Climate, 29 Jun−3 Jul, Yokohama. <www.ide.titech.ac.jp/~icuc7/extended_ abstracts/ pdf/385055-1-090515165722-002.pdf> 3.11.2013.

Strahler A. and Strahler A. (2006) Introducing Physical Geography. 4th edition. 728 pp. Wiley, New Jersey.

Streutker D.R. (2003) Satellite-measured growth of the urban heat island of Houston, Texas. Remote Sensing of Environment 85: 282–289.

Summers P. W. (1965) An urban heat island model: its role in air pollution problems, with application to Montreal. Paper1st Canadian Conf. on Micrometeorology. Toronto, nt. 12th–14th April.

Sundborg A. (1951) Climatological studies in Uppsala. Geographica No. 22. Uppsala University, Dept of Geography.

Svensson M. and Eliasson I. (2002) Diurnal air temperatures in built-up areas in relation to urban planning. Landscape and Urban Planning 61: 37–54.

Svensson M., Eliasson I. and Holmer B. (2002) A GIS based empirical model to simulate air temperature variations in the Göteborg urban area during the night. Climate Research 22: 215–226.

Szegedi S. and Kircsi A. (2003) The development of the urban heat island under various weather conditions in Debrecen, Hungary. Proceedings ICUC-5. Fifth International Conference on Urban Climate. University of Lodz, Poland. < http://nargeo.geo.uni.lodz.pl/~icuc5/> 19.12.2013.

Szymanowski M. and Kryza M. (2009) GIS-based techniques for urban heat island spatialization. Climate Research 38: 171–187.

Szymanowski M. and Kryza M. (2011) Application of geographically weighted regression for modelling the spatial structure of urban heat island in the city of Wroclaw (SW Poland). 1st Conference on Spatial Statistics: Mapping Global Change. Procedia Environmental Sciences 3:87–92.

Szymanowski M. and Kryza M. (2012) Local regression models for spatial interpolation of urban heat island – an example from Wrocław, SW Poland. Theoretical and Applied Climatology 108:53–71.

Taha H. (1997) Urban climates and heat islands: albedo, evapotranspiration, and anthropogenic heat. Energy and Buildings 25(2): 99–103.

Terjung W. and Louie S.F. (1973) Solar radiation and urban heat island. Annals of the Association of American Geographers 63(2): 181–207.

Thorsson S., Lindberg F., Björklund J., Holmer B. and Rayner D. (2011) Potential changes in outdoor thermal comfort conditions in Gothenburg, Sweden due to climate change: the influence of urban geometry. International Journal of Climatology 31:324–335.

Tsangrassoulis A. (2001) Short-wave radiation. In Santamouris, M. (ed.), Energy and Climate in the Urban Built Environment. 229 pp. Cromwell Press, UK.

Tumanov S., Stan-Sion A., Lupu A., Soci C. and Oprea C. (1999) Influences of the city of Bucharest on weather and climate parameters. Atmospheric Environment 33: 4173–4183.

Unger, J. (1996) Heat island intensity with different meteorological conditions in a medium-sized

town: Szeged, Hungary. Theoretical and Applied Climatology 54: 147-151.

Unger J., Sümeghy Z., Gulyás Á., Bottanyán Z. and Mucsi L. (2001) Land-use and meteorological aspects of the urban heat island. Meteorological Applications 8: 189–194.

Unger J., Savić S. and Gál T. (2011) Modelling of the annual mean urban heat island pattern for planning of representative urban climate station network. Advances in Meteorology. Article ID: 398613, 9 pages. DOI: 10.1155/2011/398613

Unwin D.J. (1980) The synoptic climatology of Birmingham's urban heat island, 1965–1974. Weather 35: 43–50.

Upmanis H., Eliasson I. and Lindvist S. (1998) The influence of green areas on noctural temperature in a high latitude city (Göteborg, Sweden). International Journal of Climatology 18: 681–700.

Vaneckova P., Hart M.A., Beggs P.J. and de Dear R.J. (2008) Synoptic analysis of heat-related mortality in Sydney, Australia, 1993–2001. International Journal of Biometeorology 52: 439–451.

Vardoulakis E., Karamanis D., Fotiadi A. and Mihalakakou G. (2013) The urban heat island effect in a small Mediterranean city of high summer temperatures and cooling energy demands. Solar Energy 94: 128–144.

Voogt J.A. and Oke T.R. (2003) Thermal Remote Sensing of Urban Climates. Remote Sensing of Environment 86: 370–384.

Wen X., Yang X. and Hu G. (2011) Relationship between land cover ratio and urban heat island from remote sensing and automatic weather stations data. Journal of the Indian Society of Remote Sensing 39: 193−201.

Weng Q. (2009) Thermal infrared remote sensing for urban climate and environmental studies: methods, applications, and trends. ISPRS Journal of Photogrammetry and Remote Sensing 64: 335–344.

WHO (2013) World Health Organization. >http://www.who.int/en/> 16.11.2013.

Wienert U. and Kuttler W. (2005) The dependence of the urban heat island intensity on latitude – a statistical approach. Meteorologische Zeitschrift 14(5): 677–686.

Wilby R.L. (2003) Past and projected trends in London's urban heat island. Weather 58: 251–260.

Wypych A. (2010) Twentieth century variability of surface humidity as the climate change indicator in Kraków (Southern Poland). Theoretical and Applied Climatology 101: 475–482.

Yamashita S. (1996) Detailed structure of heat island phenomena from moving observations from electric tram-cars in metropolitan Tokyo. Atmospheric Environment 30: 429–435.

Yokobori T. and Ohta S. (2009) Effect of land cover on air temperatures involved in the development of an intra-urban heat island. Climate Research 39: 61–73.

Zhang N. and Chen Y. (2013) A case study of the upwind urbanization influence on the urban heat island effects along the Suzhou–Wuxi Corridor. Journal of Applied Meteorology and Climatology 53: 333–345.